Vol. 503: 75–97, 2014
doi: 10.3354/meps10725

MARINE ECOLOGY PROGRESS SERIES
Mar Ecol Prog Ser

Published April 29

Individual-based modelling of *Calanus sinicus* population dynamics in the Yellow Sea

Luning Wang[1], Hao Wei[2,*], Harold P. Batchelder[3]

[1]College of Physical and Environmental Oceanography, Ocean University of China, Qingdao 266100, PR China
[2]College of Marine Science and Engineering, Tianjin University of Science and Technology, Tianjin 300457, PR China
[3]College of Earth, Ocean and Atmospheric Sciences, Oregon State University, Corvallis, OR 97331-5503, USA

ABSTRACT: *Calanus sinicus* is the dominant copepod species in the coastal waters of China. We studied its population dynamics using an individual-based model (IBM) based on physiological processes at the individual level. The model includes modules describing development, growth, reproduction, mortality, diel vertical migration and diapause. Development, growth and reproduction are affected mainly by temperature and food concentration. Mortality includes routine mortality of stage plus density-dependent mortality, and weight-dependent mortality for N1–C6 stages. Control of seasonal diapause is based on lipid accumulation and lipid metabolism. The model was applied in a 1-dimensional water column located in the central Yellow Sea, and simulations showed that the population of *C. sinicus* peaks twice in 1 yr, with the earlier peak depending strongly on the phytoplankton bloom in spring, and the later (December) peak relying on lipid-stored energy from the over-summering population dominated by diapausing C5s. The model population of *C. sinicus* goes through 3 generations in 1 yr, and the over-summering population of diapausing C5s consists of both first (G1) and second (G2) generation individuals. Coupled with more extensive field observations of abundance and biomass of *C. sinicus*, an IBM can be forced using output from an integrated hydrodynamic-nutrient-phytoplankton model to examine the processes responsible for the spatial-temporal variation of *C. sinicus* throughout its range in the Yellow Sea.

KEY WORDS: Individual-based model · *Calanus sinicus* · Population dynamics · Diapause · Lipids · Yellow Sea

INTRODUCTION

Zooplankton are considered as secondary producers in the marine food web, and their population dynamics could affect the populations of phytoplankton and fish. Copepods, as the numerically dominant grazers of the mesozooplankton, play an important role in energy flow from low to high trophic levels in the food web. Physiological processes and behaviors of different life stages of copepods may differ greatly, so it is important to consider the role of these life-stage dependent differences when simulating copepod population dynamics (Batchelder & Williams 1995). In addition, the mechanisms of how physical and biological processes affect populations of copepods are critical to understanding marine ecosystem dynamics.

The Yellow Sea is a unique marine ecosystem in East China Seas, with a mean depth of 44 m. Two prominent physical features of the Yellow Sea are (1) the persistence in summer of cold bottom water with a mean temperature of 8 to 10°C in the central Yellow Sea — hereafter referred to as the Yellow Sea Cold Bottom Water (YSCBW) (Ho et al. 1959, Kwan 1963, Su & Weng 1994, Su 2001, Zhang et al. 2008); and (2) the presence in winter of the Yellow Sea

*Corresponding author: weihao@ouc.edu.cn

Warm Current (YSWC), with temperatures in the range of 10 to 17°C (Kwan 1962, Weng et al. 1988, Teague & Jacobs 2000, Tang et al. 2001). The spring phytoplankton bloom in the southern Yellow Sea, associated with peak chlorophyll *a* (chl *a*) concentrations, occurs in March or April (Liu 2010).

Calanus sinicus is an abundant planktonic copepod widely distributed in the coastal waters of China and Japan, and it was selected as a target species for ecosystem dynamics studies in the Yellow Sea by the China Global Ocean Ecosystem Dynamics (GLOBEC) program (Wang et al. 2003). During research programs initiated in 1999 and 2005, substantial progress was made on understanding the physiology (Zhang et al. 2000, Zhang 2001, Pu et al. 2002, Wang et al. 2002), ingestion (Li C et al. 2004, Li J et al. 2006), reproduction (Zhang F et al. 2002a, 2002b), population recruitment (Zhang G et al. 2005, Wang 2009), oversummering strategy (Sun et al. 2002, Pu 2003, Wang et al. 2003, Pu et al. 2004b), and diapause and lipid accumulation (Wang 2009, Sun et al. 2011a) of *C. sinicus*. These investigations showed that *C. sinicus* comprises a mean fraction of 50% in abundance and 80% in biomass (Yang & Xu 1988) of zooplankton in the Yellow Sea. In the Yellow Sea, the population of *C. sinicus* completes 3 to 4 generations per year (Chen 1964, Wang 2009). In March or April, the population appears to be most abundant in regions near the coast that have high primary production and in frontal zones with high temperature gradients. Abundances are highest in May or June (Zhang G et al. 2005). With the increasing temperatures in coastal waters during summer, the center of the *C. sinicus* population transitions from the coast to the central region of the Yellow Sea where the deep YSCBW provides a thermal refuge from the excessively warm surface temperatures (Sun et al. 2002, Wang et al. 2003). In summer, *C. sinicus* can hardly survive above the thermocline due to the high temperatures, and the population consists almost exclusively of diapausing Stage C5 copepodites (hereinafter also referred to as 'C5s'; see further explanation of life stages in the description of the model below) in the YSCBW. Diapausing individuals at <10°C have low metabolic rate (Li et al. 2004), cease feeding, diel vertical migration (DVM) and development (Pu et al. 2004b), and maintain themselves using stored lipid reserves (Wang 2009, Sun et al. 2011a). From late October or November, the YSCBW disappears as a temperature-salinity (T-S) differentiated water mass due to vertical mixing, and the *C. sinicus* C5s terminate diapause and mature into adults for reproduction, creating a second period of *C. sinicus* population increase (Chen 1964). During this time the copepods disperse in surface waters over much of the Yellow Sea (Yin et al. 2013).

Therefore, the YSCBW plays an important role as a refuge from the high surface temperatures in summer that permits survival and eventual recruitment of *Calanus sinicus* in winter. Also, the oversummering diapause at relatively cold near-bottom temperatures allows energy (lipid) stores accumulated from ingestion of phytoplankton during the spring bloom to be transferred directly into early winter reproduction (Jónasdóttir 1999). Here we develop a population dynamics model to examine the mechanisms and processes that influence the population dynamics of *C. sinicus* and enable it to succeed through an extended summertime period of unfavorable conditions.

Traditional ecosystem models often adopt a bulk biomass-based approach to simulate important functional groups, such as nutrients, phytoplankton, zooplankton and grazers in marine systems. Such models can successfully simulate carbon or nutrient budgets and cycling in the ocean, but have limited capacity compared to life-history based models that include unique aspects of the life cycle that may be needed to survive in marginal habitats. This is especially true for some zooplankton and fish species, which have complex life histories and physiologies that are controlled directly or indirectly by behaviors that may vary with life stage. Aggregated biomass type models cannot adequately capture the features of short-term behavioral or physiological responses of species, which are likely represented in the composition or structure rather than the biomass of the population (Heath et al. 1997). An individual-based model (IBM) incorporates life history details and can accommodate the responses of individual physiological activities to environmental changes and their effects on growth, metabolic processes, mortality, and ultimately population dynamics. Because of this, the IBM approach has been widely used in population dynamics models of zooplankton and fish (Miller 2007, North et al. 2009, Neuheimer et al. 2010).

Batchelder & Williams (1995) developed an IBM of *Metridia lucens*, a copepod in the North Atlantic Ocean, based on an earlier model for a congener in the North Pacific (Batchelder & Miller 1989). The results showed that by taking into consideration both individual-specific factors (size, ingestion history, behavior) and environmental factors (temperature, food) simultaneously, an IBM can simulate the seasonal variability of population composition.

For zooplankton populations, reproduction and survival determine population recruitment. Carlotti & Hirche (1997) developed an IBM of *Calanus finmarchicus* females that includes physiological responses to intermittent short-term food limitation on growth and egg production. By coupling an IBM of *C. finmarchicus* to a regional circulation model of the Gulf of Maine and Georges Bank, Miller et al. (1998a) provided insights on the sources of diapausing individuals that contribute to the seasonal development of *C. finmarchicus* in surface waters of the Gulf of Maine and repopulation of Georges Bank.

DVM is an important physiological and behavioral action for many copepods, which is related to variation in food, temperature, predator pressure and light intensity. Batchelder et al. (2002) demonstrated the strong influence of behavior and physiology on spatial distributions and reproduction, using a copepod IBM that includes ontogenetically-determined amplitudes of DVM interacting with the 2-dimensional coastal upwelling circulation. The DVM of individuals in that model was determined by light intensity, individual size, food concentration and physiological condition (hunger). Comparisons of simulation results with and without ontogenetic-DVM showed dramatic differences in nearshore retention and spatial distributions over a 120 d period during summer upwelling.

Many copepods have a metabolically reduced state (diapause) at depth, where temperatures are cooler and food is scarce, to withstand adverse surface environmental conditions, such as high temperatures and low food concentrations. During diapause, animals cease development, reproduction and ingestion and have reduced metabolic demands (Ohman et al. 1998, Hind et al. 2000). However, the exact mechanism that triggers the initiation and termination of diapause is uncertain. In addition to hypotheses of photoperiod (Miller et al. 1991)—now generally disproved (Hind et al. 2000)—and food-limited control (Hind et al. 2000), the hypothesis of lipid control has garnered attention in recent years (Lee et al. 2006, Johnson et al. 2008, Maps et al. 2010, 2012). Maps et al. (2010) were the first to apply an approach based entirely on lipid accumulation and metabolism for the control of diapause in an IBM of *Calanus finmarchicus*, which was developed from Fennel's (2001) study. To simulate diapause, they assumed that the active C5s enter diapause when the ratio of lipid to weight exceeds a threshold value, and the diapausing C5s awaken when the ratio decreases below a lower threshold value.

Using details known about the life history and physiological processes of *Calanus sinicus*, we developed an IBM to simulate the development, growth, reproduction, DVM and diapause of many individuals. The goal was to reproduce in aggregate the observed seasonal variations of abundance, biomass, and stage composition at the population level. Sensitivity analyses were conducted to test some parameterizations of the model, in order to identify aspects of the ecology and physiology of *C. sinicus* where further knowledge might improve the representation of the species' population dynamics. Further work is needed to couple the IBM with a hydrodynamic and nutrient-phytoplankton model, in order to better understand the full suite of processes that control the timing, spatial patterns and abundances of *C. sinicus* throughout the Yellow Sea.

DESCRIPTION OF THE MODEL

Frame of the model

Based on key vital rates and processes of the life history of *Calanus sinicus*, the present model is divided into modules describing development, growth, reproduction, mortality, diapause and DVM. The functions and parameters are shown in Supplements 1, 2 & 3 at www.int-res.com/articles/suppl/m503p075_supp.pdf. A time step of 2 h was used for all IBM simulations.

Due to the huge number of individuals in a natural copepod population, it is difficult to simulate every individual under present computational constraints. In order to reduce computational complexity, the 'superindividual' is introduced into the model (Schef-

Table 1. *Calanus sinicus.* Components of state vectors for a superindividual tracked by an individual-based model (IBM) at each time step. nd: non-dimensional

Life stage (nd)
Development progression (nd)
Generation (nd)
Sex ratio (nd)
Oil sac volume ratio (%)
The factor that represents diapause (nd)
Number of egg clutches produced by females (nd)
Structural weight of an individual (µg C)
Oil sac weight of an individual (µg C)
Reproductive weight of an individual (µg C)
Number of individuals represented by the superindividual (ind.)
Depth (m)

fer et al. 1995), which consists of a subset of individuals having identical attributes that are tracked through space and time as a single entity (Table 1). Life stage attributes of copepods, for example, can be represented by integers that range from 1 to 15, encompassing a life cycle from egg to adult. In the present study the life stages are described as follows: egg, 6 naupliar stages (N1 to N6), 5 active immature copepodite stages (C1, C2, C3, C4,and C5a), a diapausing C5 stage (C5d), adult males (C6m) and adult females (C6f). Other attributes, such as individual carbon mass or fraction of development (FD) completed, are real numbers that change more continuously, and possibly bidirectionally during simulations. In addition, an attribute is used to indicate the number of identical individuals represented by the superindividual; this attribute may decrease as time advances due to mortality experienced by the individuals within the superindividual. The male:female sex ratio of immature stages of *Calanus sinicus* in this model is assumed to be 1:1, and vital rates of immatures are assumed to be independent of sex. When the stage attribute of a superindividual matures to the adult stage, 50% of the individuals within the superindividual are transferred to a newly created superindividual that has all attributes identical to the source superindividual, except the stage is set to C6m (adult males). The remaining individuals that remain in the source superindividual are assigned a stage of C6f (adult females). Subsequently the adult male and female superindividuals have independent attribute dynamics and trajectories. If a superindividual's weight is reduced below a critical weight threshold for survival or the number of individuals represented by a superindividual falls to zero, then the superindividual is deleted from the model and is no longer tracked. At each time step, each C5a superindividual is evaluated against criteria described below to determine whether it transitions into the C5d (diapausing) stage. Similarly, C5d superindividuals in diapause awake and become adults based on a different set of physiological criteria discussed below. Transitions into and out of diapause are irrevocable for a given superindividual. Beyond the initial superindividuals at the start of a simulation, new superindividuals are created only by splitting of C5a or C5d individuals into separate sexes at maturation, and by reproduction, which create new superindividuals of eggs. Hereafter, we use the terms 'superindividual' and 'individual' interchangeably. The flowchart of the IBM processes and decision (break points) in the model are shown in Fig. 1.

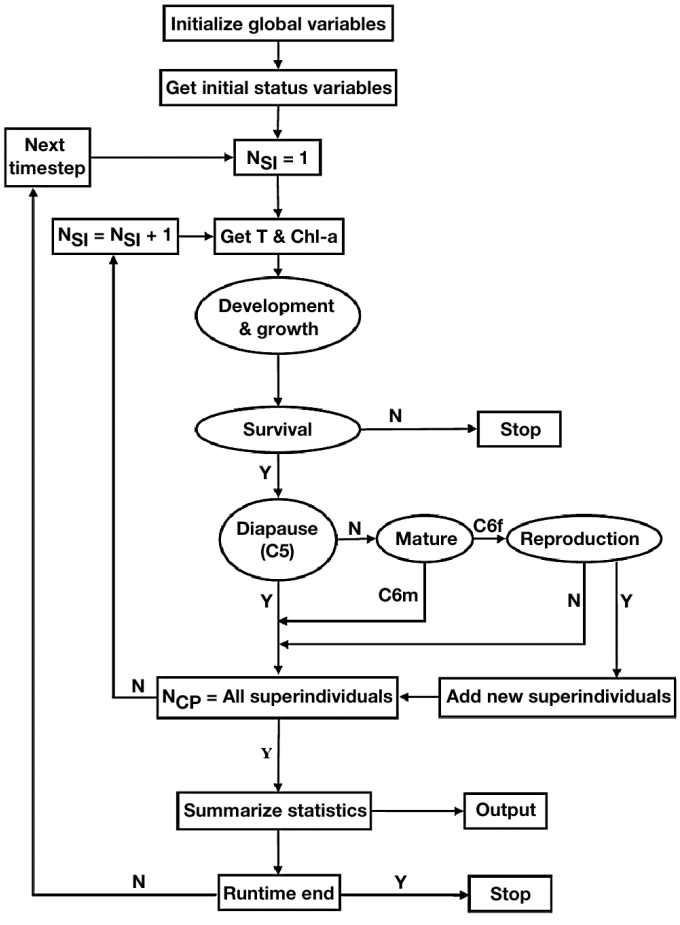

Fig. 1. Flowchart of the individual-based model (IBM) for *Calanus sinicus*

Development

Based on experiments conducted with surplus food conditions (Uye 1988), the development time of *Calanus sinicus* as a function of temperature is approximated well using the Belehrádek function (McLaren et al. 1969):

$$D_i = \beta_i (T + T)^{\theta_b} \quad (1)$$

where D_i is the duration (d) from egg laying to the beginning of stage i, T is the temperature, β_i is a stage dependent constant, and T_b and θ_b are constants (see Supplements 1 & 2). Temperature-dependent stage-duration (SD) is calculated, for example, as $SD_{C3} = D_{C4} - D_{C3}$ for C3, and similarly for all the other stages. At constant temperature, the development of individuals in different stages follows the equiproportional rule (Fig. 2). Food concentration also affects development time in copepods (Vidal 1980, Campbell et al. 2001, Ohman &

Hsieh 2008, Record & Pershing 2008, Pershing et al. 2009). The Belehrádek function is modified to include an Ivlev-type ingestion function to account for this (Johnson et al. 2008; see Supplements 1 & 2).

Each superindividual includes an attribute in the state vector that tracks the progression of an individual through a life stage, FD, equivalent to the molt cycle fraction of Miller & Tande (1993). When the individual first enters stage *i*, FD is set to 0, and it will be increased by $\Delta t/SD_i$ in Δt. When FD is greater than or equal to 1, the individual is molted into the next stage $i+1$, and the value of FD is reset to 0.

Growth

Individual growth (G), expressed as the change in carbon weight (µg C) per unit time, is dependent on the rates of assimilation (A) and respiration (R): G = A – R. Within an individual, growth may be partitioned into compartments that represent structural body mass (W_S), oil (lipid) reserves (W_O) or gonads (eggs) (W_E). Assimilation is dependent on ingestion (I) which is a function of food concentration, individual body mass and temperature (see Supplement 1). Food concentration effects on *Calanus sinicus* feeding stages (N3 to C6) are described by a Michaelis-Menten function fit to adult female ingestion (Huo et al. 2008; Fig. 3). Stage-specific adjustments to I_{max} (= 14.8 for adult females), using the scale parameter $\varphi_{I,i}$, are used to balance ingestion and respiration to match observed experimental measures of growth (e.g. weight at stage) as described below. Temperature effect on ingestion is implemented with a van't Hoff (Q_{10}) function (Thornton & Lessem 1978). An allometric function is used to adjust maximum ingestion by individual body mass (see Supplements 2 & 3; www.int-res.com/articles/suppl/m503p075_supp.pdf). Individual respiration (R) is a function of temperature and weight, based on the oxygen consumption rates (R_{O2}) of copepods (Ikeda et al. 2001; Supplement 1). For zooplankton, the value of the respiratory quotient (q) is set to 0.97, and reduces to 0.72 if the metabolic substrate is lipid instead of carbohydrates (Gnaiger 1983). The factor 12/22.4 represents the carbon weight per mole of CO_2. The scale parameters for ingestion ($\varphi_{I,i}$) and respiration (φ_R) are used to match simulated *C. sinicus* growth (e.g. individual size) using independently derived ingestion (Huo et al. 2008) and respiration (Ikeda et al. 2001) functions to the experimentally observed growth of *C. sinicus* (Uye 1988). For further explanation see the section 'Parameter tuning' below.

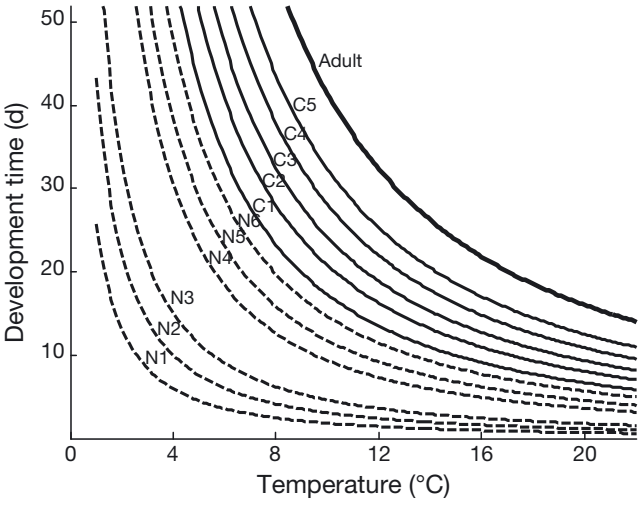

Fig. 2. *Calanus sinicus*. The relationship of temperature and development time (d) from egg laying to each stage under excess food condition after Uye (1988). N1 to N6: naupliar stages; C1 to C5: copepodite stages. Dashed lines: from egg to nauplii stages; solid lines: from egg to copepodite stages; bold solid line: from egg to adult

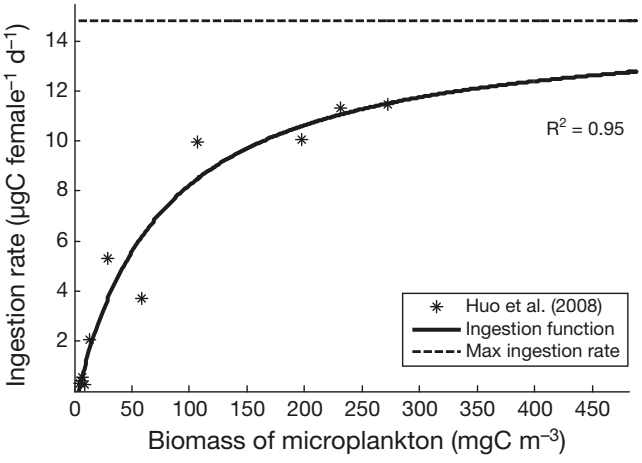

Fig. 3. *Calanus sinicus*. The relationship between ingestion rate by females (µg C d^{-1}) and biomass of microplankton (mg C m^{-3}). Asterisks: data from Huo et al. (2008); solid line: fitted Michaelis-Menten ingestion function; dashed line: fitted I_{max}; R^2: correlation coefficient

Diapause

In summer when surface mixed layer temperatures exceed 20°C, the population of *Calanus sinicus* concentrates in YSCBW, mainly as C5s in diapause (Sun et al. 2002). This allows some individuals to survive a period when the combination of high mixed layer temperature and low food concentration are likely to be lethal, and subsequently to mature and reproduce during cooler autumn conditions. The model adopts

an approach based on the hypothesis that lipid accumulation and metabolism of *C. sinicus* C5s are important in the control of diapause, as suggested previously for other *Calanus* spp. (Lee et al. 1970, 2006, Miller et al. 1998b, 2000, Rey-Rassat et al. 2002, Irigoien 2004). Because *C. sinicus* C5s are rarely observed in upper mixed layer waters of the central Yellow Sea during the warmest summer stratified period (Wang et al. 2003), we require also that C5 stages actively avoid the surface mixed layer when there is strong subsurface stratification ($\delta T/\delta z \geq 0.2$°C m^{-1}) and surface $T \geq 20$°C. Exclusive of mortality, C5a individuals have 3 possible fates: (1) under favorable temperature conditions they mature from C5a to C6 (when $\delta T/\delta z < 0.2$°C m^{-1} and $T < 20$°C), or (2) they immediately transition from C5a to C5d (when $\delta T/\delta z \geq 0.2$°C m^{-1} and $T \geq 20$°C), or (3) they undergo a lipid controlled transition from C5a to C5d (when $\delta T/\delta z \geq 0.2$°C m^{-1}, $T < 20$°C, and a third condition, $OSV_{ind} \geq \lambda_{max}$, is also satisfied as explained below). For this transition process, we include functions that govern the partitioning of growth into structural tissues and lipid storage. The implemented algorithm assumes that lipid is accumulated between C3 and C5 (Kattner & Krause 1987, Hygum et al. 2000) when the growth rate (G) is positive. At each time step having positive growth, a fraction of carbon, f_{oil}, is partitioned into lipid stores (see Supplements 1 & 2). To be consistent with the observations of lipid/body volumes in *C.sinicus* (Wang 2009, Sun et al. 2011a), an oil storage volume ratio (OSV) is used to quantify the approach to entering diapause. C5a individuals that attain an OSV exceeding a critical threshold of λ_{max} will transition from C5a to C5d if the vertical temperature (thermocline) gradient threshold is exceeded. At the transition to diapause, C5d individuals adopt reduced metabolic rates (supported from the lipid stores), cease ingestion and developmental progress and descend to a randomly selected depth between the bottom and the thermocline and discontinue DVM excursions to the surface waters. Diapause will terminate when the strong thermocline disappears or the OSV_{ind} decreases below the minimum threshold λ_{min}. In *C. finmarchicus*, production of eggs by adult females may be supported by residual lipid stores remaining after maturation (Jónasdóttir 1999, Rey-Rassat et al. 2002, Irigoien 2004). We assume also that upon maturation, adult females of *C. sinicus* convert residual lipid stores into the gonad with an efficiency, f_{O2E}, of 0.5 (50%; Jónasdóttir 1999). This enables newly matured females from C5d to produce a clutch of eggs shortly after maturation, even in unfavorable (e.g. low food) environments.

The oil storage volume ratio is obtained from the oil sac volume and the body volume (Supplement 1). The oil sac volume (V_{oil}) is calculated from the wet weight of lipid stores ($W_{W,oil}$), which is converted from carbon that is directed into oil storage, and the density (ρ_{oil}) of lipid (Miller et al. 1998b, Lee et al. 2006, Saumweber & Durbin 2006). In the model, individuals are assumed to be ellipsoidal in shape, and the body volume (V_l) is calculated as in Wang (2009) (Supplement 1). *Calanus sinicus* body length (L_p) is calculated from weight using the result from Uye (1988), and the maximum width of the body (d) is assumed to be a fraction (f_{d2l}) of body length.

Reproduction

Within an adult female the mass of structural tissues ($W_{C,S}$) and mass of gonads ($W_{C,E}$) are tracked independently. The fraction of new growth allocated to gonad, f_E, is an increasing function of adult female mass (see equation in Supplement 1: Reproduction), such that smaller females have greater allocation to somatic increase than do larger females, which direct more growth into egg production.

Whether a clutch of eggs is laid on any given night after a female matures depends on the amount of carbon accumulated for egg production, (i.e whether $W_{C,E}$ exceeds or equals the minimum gonad weight allowing reproduction by an adult female ($W_{C,E0}$), the temperature (which affects the efficiency of conversion of stored carbon into eggs; e_{EP}), and a random effect. The random component provides for variation in clutch size (e.g. prevents the clutches from all being close to the minimum possible size) by creating a 24 h delay before the next laying opportunity. The random effect is implemented by generating a random normal variate $N(\mu, \sigma^2)$ for each reproductive female at midnight, where μ and σ^2 are the mean and variance, respectively, of clutch size. A female will release a clutch if the generated random clutch size requires less carbon than the female has available for eggs. Eggs produced by all of the females in the parent superindividual are aggregated into a new superindividual of stage egg in the model.

Observations of clutch sizes from *Calanus sinicus* in the Inland Sea of Japan in April and June were used to estimate μ and σ^2 (Uye & Murase 1997; Fig. 4). Results from recent springtime measures of *C. sinicus* clutch size in the Yellow Sea are similar (Kang et al. 2011, Li et al. 2013, Wang et al. 2009). In the present model, egg production rate is assumed to follow the April results when surface temperature

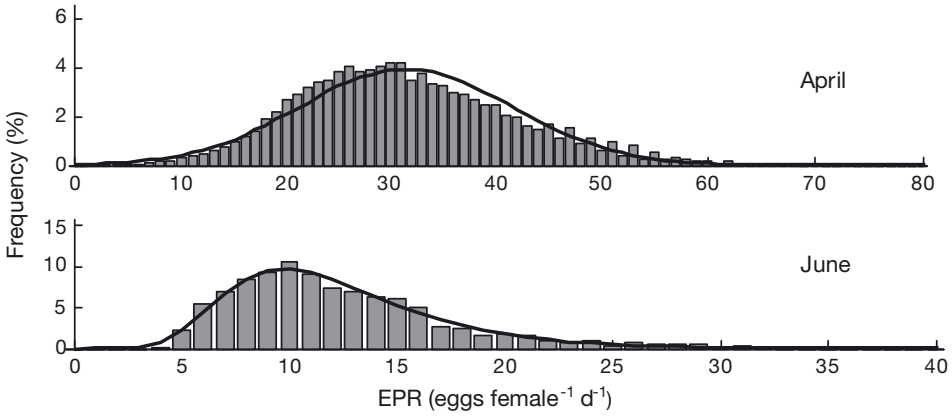

Fig. 4. *Calanus sinicus.* Frequency distribution of clutch size (no. of eggs per clutch) of females in April and June in the Inland Sea of Japan (Uye & Murase 1997)

is <15°C, and the June results when temperature is ≥15°C. An individual female may produce a maximum of $N_{EP,max}$ clutches during her lifetime.

Mortality

Mortality is an important control on the population dynamics of zooplankton, and is affected by temperature, food, predation pressure and population density. However, field rates of mortality are difficult to estimate so rates applied to models are often poorly constrained by observations. Here we make assumptions about the sources and relative magnitudes of mortality.

In the life history of *Calanus sinicus*, the survival of the egg stage is considered as the most vulnerable period (Zhang G et al. 2002b). A density-dependent effect of *C. sinicus* C5 and adult female cannibalism on eggs is considered using a linear function of the depth-integrated abundance (ind. m^{-2}) of females and C5s (Maps et al. 2010, 2011).

For naupliar (N1 to N6) and copepodite (C1 to C5) stages, mortality arises from 3 factors: a basal (routine) mortality, a starvation-enhanced mortality and an abundance-enhanced mortality. Routine mortality, $M_{R,i}$, is independent of environmental factors, but may differ by stage (naupliar, immature copepodites and adults) as implemented in previous IBMs (Batchelder & Miller 1989, Batchelder & Williams 1995). We set the value of $M_{R,i}$ of the 3 stage groups, i.e. the routine mortalities of nauplii (M_N), immature copepodites (M_C), and adult females (M_A) between 0.005 and 0.05 d^{-1}. Starvation mortality, $M_{starv,i}$, equal to $M_{R,i}$ (effectively doubling routine mortality) occurs when the weight of an N3 to C6 individual declines below a stage- and temperature-specific threshold weight, $W_{starv,i}$. The increase in mortality due to intraspecific competition for food, $M_{abun,i}$, is based on the depth-integrated abundance of individuals within the specific stage-grouping as described in Maps et al. (2011) (see Supplement 1 for mortality equations; Supplements 2 & 3 for mortality-related parameter values). In addition, the routine mortality rate of adult males is assumed to be twice that of adult females, and the routine mortality rate of C5s in diapause is assumed to be only 10% of the routine rate of the active C5s (Maps et al. 2010).

At every time step, the number of individuals represented by a superindividual is reduced exponentially: $N_{t+\Delta t} = N_t\, e^{-M\cdot\Delta t}$ (Fager 1973), where total mortality $M = M_R + M_{starv} + M_{abun}$. A superindividual is removed from further model calculations if it no longer represents at least 0.5% of the initial number it represented, or if the mean individual weight it represents decreases to zero.

Diel vertical migration

Calanus sinicus copepodites perform DVM, which is especially prominent for C5 and female stages (Cheng et al. 1965, Liu & Wang 1991, Zhang F et al. 2005). In the model, *C. sinicus* C1 to C6 individuals (except C5d) migrate vertically between the surface (at night; ~21:00 to 03:00 h local time) and near bottom (during daylight; ~06:00 to 18:00 h local time), except during summer periods when there is very strong vertical thermal stratification in the YSCBW, with surface temperatures >20°C, and when the copepodites only migrate upwards at night to depths near the base of the thermocline, where they may aggregate. Diapausing C5s remain in YSCBW at temperatures <10°C, and do not perform DVM. In the model, DVM is implemented very simply by assuming a 3 h period of transition (18:00 to 21:00 h local time) from the deep daytime depth to a shallower nighttime depth, and similarly from 03:00 to

06:00 h local time for transitioning from surface to deep depth near dawn. For the downward transition, a depth between 5 m above the bottom and 50 m below the surface is randomly selected and the individual moves linearly over the 3 h to that depth, where it remains for all of the following daytime period. A similar approach is used to move individuals to randomly selected shallower daytime depths between 0 and 30 m when the strong thermocline is absent. After the strong thermocline develops (e.g. from late June to mid October), the depth for nighttime feeding is randomly selected between the base of the thermocline and 40 m depth. As in the daytime deep duration, the nighttime shallow duration continues for the full night at the randomly selected depth between 5 m above the bottom and 50 m. However, each successive day a given particle receives independent day and night depths.

SIMULATIONS FOR PARAMETER ESTIMATION

A series of simulations are carried out to establish some of the less known parameters in the model, or to reconcile potential discrepancies that arise from using bioenergetic functions that originate from many different studies done in different ocean regions. An example of the latter is the reconciliation of ingestion and respiration functions, so that together they satisfactorily replicate growth trajectories from youngest to adult stages of *Calanus sinicus* in laboratory rearing experiments. An example of the former is the establishment of reasonable lipid accumulation rates and lipid thresholds, such that the timing and duration of diapause are close to the observed seasonal timing for the Yellow Sea, and the lipid storage levels are consistent with observations of lipid contents in field collected individuals. These parameter estimation simulations are presented below, and provide key values for parameters that are used in subsequent simulations of *C. sinicus* dynamics in the central Yellow Sea throughout an annual cycle (see 'Application of the Model' below).

Growth in food-replete conditions

The objective of this exercise is to use the detailed observations of *Calanus sinicus* growth made by Uye (1988) in temperature controlled and closely monitored experimental conditions. The *C. sinicus* were collected from the Inland Sea of Japan rather than the Yellow Sea, but comparable experiments using Yellow Sea *C. sinicus* have not been done. The Uye (1988) experiments done at 5 temperatures ranging from 10.3 to 20.2°C are clearly the best measurements of *C. sinicus* growth throughout the entire life cycle under known conditions of temperature and food availability. Cultured phytoplankton provided to *C. sinicus* during these experiments were either diatoms (naupliar stages) or a mix of diatom and dinoflagellates (copepodites), and food concentration was maintained at a minimum of 900 µg C l^{-1}, to keep food in excess. The experiment simulated growth of individuals from egg to C6 with the initial egg weight set to 0.2 µg C (Uye & Marase 1997).

The parameters to be adjusted in harmonizing the processes of ingestion, respiration, and growth in this exercise are the non-dimensional stage-specific coefficients, $\varphi_{I,i}$, that scale ingestion, and a single non-dimensional coefficient, φ_R, that scales respiration identically for all life stages. We scaled stage-specific ingestion in order to match the simulated weights at every life-stage with the observations of Uye (1988) for all 5 temperatures. For consistency, the $\varphi_{I,i}$ coefficients are shown for all non-egg stages (Supplement 3), even though they are not required for the non-feeding N1 and N2 (these were set to zero). For these simulations we assume that the dependence of development rates on temperature (stage progression) is accurately described by the Belehrádek functions described earlier. In initial simulations of development and weight histories, $\varphi_{I,i}$ and φ_R are assumed to be 1.0. These coefficients are adjusted iteratively beginning with the younger life stages, since the weights of the older life stages are a cumulative effect of the growth (and size) of the earlier stages. The initial simulation (not shown) consistently and slightly underestimates the weight at stage of all of the feeding naupliar stages; naupliar stage weights are brought into balance by reducing φ_R from the initial 1.0 to 0.8. We then establish values for $\varphi_{I,i}$ for each copepodite stage sequentially from youngest to oldest. Fig. 5 shows the comparison of weight at stage for active stages N2 to C5 for $\varphi_R = 0.8$, and the values of $\varphi_{I,i}$ listed in Supplement 3. The root mean square (RMS) between the simulations and the observations, standardized by the mean weights from observations, is adopted to determine the appropriate parameters. Additional combinations of these parameters are tested using ad hoc and intuitive changes to parameters, but they do not provide better matches of simulated and experimentally observed growth trajectories at the 5 temperatures examined by Uye (1988). We do not conduct an exhaustive systematic search for the single parameter set that would mini-

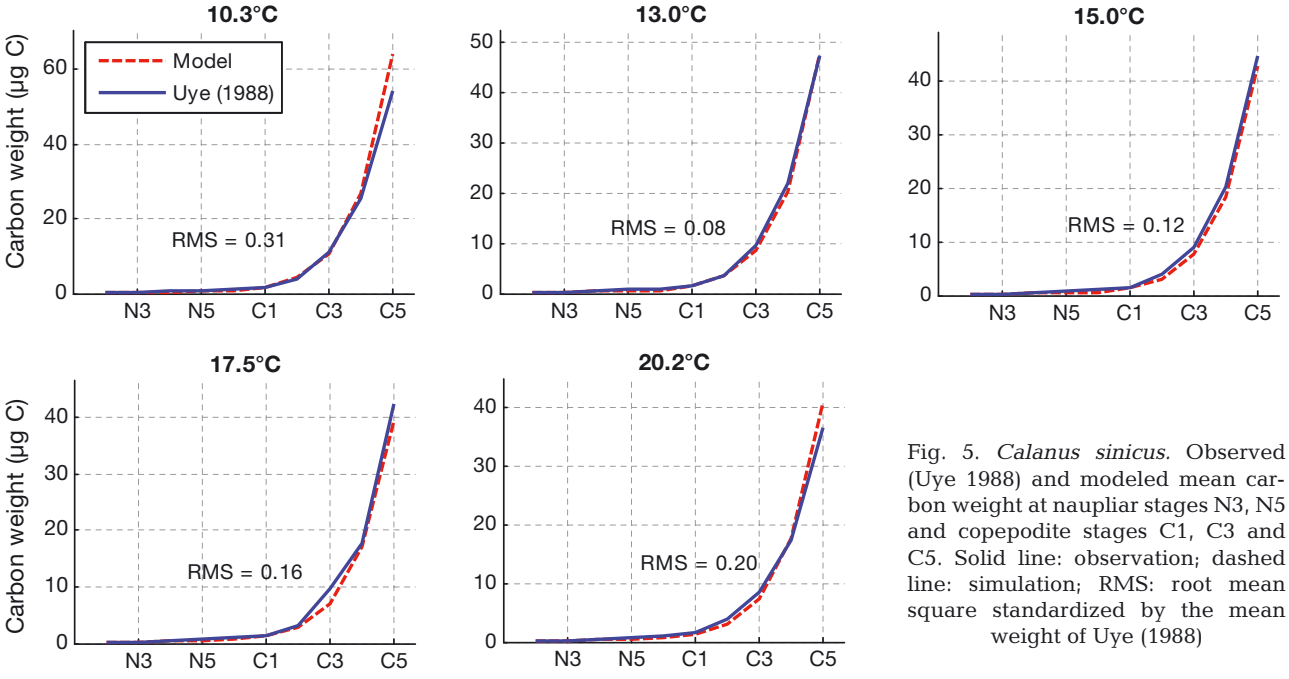

Fig. 5. *Calanus sinicus*. Observed (Uye 1988) and modeled mean carbon weight at naupliar stages N3, N5 and copepodite stages C1, C3 and C5. Solid line: observation; dashed line: simulation; RMS: root mean square standardized by the mean weight of Uye (1988)

mize the sum of squared difference between model and experiment stage specific weight for all 5 temperature conditions simultaneously. We note that the model simulated weights slightly overestimate stage-specific carbon weights compared to the experiments, especially at the 2 temperature extremes (10.3 and 20.2°C).

Lipid storage and diapause

The objective of these experiments is to estimate the oil (lipid) growth rate and limiting threshold values of oil storage volume that control the beginning and ending of diapause in *Calanus sinicus* C5s. We assume that the complex lipid-dynamics control of diapause of *C. sinicus* C5s can be parameterized using relatively few parameters that we estimate by tuning a model to seasonal patterns of *C. sinicus* OSV observations of the life stages and simple assumptions of how ingested carbon is partitioned into structural biomass or lipid biomass in the older copepodite stages. We conduct 2 types of simulations related to diapause control parameter estimation. The first set of simulations relies on prior observations of seasonal variation in lipid content (OSV) of *C. sinicus* C5s in the Yellow Sea shelf regions (Sun et al. 2011a). Fig. 6 shows that OSV increases most dramatically during spring, when many C5s attain an OSV of 20 to 40%. Mean OSV is highest (~28%) in May and June, when >65% of the C5s had an OSV >20%. Thereafter, mean OSV declines to ~5% in December, and remains <6% through March, but a few *C. sinicus* are found with OSV > 20% in most months.

The OSV of C5s is determined by the lipid accumulation rate into the oil storage during the later copepodite stages (we assume during C3 to C5). For lipid accumulation to occur requires net positive growth—with some of this partitioned to somatic structural tissues, enabling the copepodites to both grow in size and develop—but also that they do not get as structurally large as possible, as some growth is directed instead to the lipid stores. The May to June period, when the spring bloom occurs in the central Yellow Sea, appears to be the only time of the year when energy is sufficient to allow significant increase in lipid stores in *Calanus sinicus*. Partitioning of lipid during C3 to C5 stages is controlled by f_{oil}, i.e. the fraction of net positive growth that is directed to oil storage instead of somatic growth. Simulations of the accumulation of oil (increase in OSV) during growth and development from C3 to C5 are done for values of f_{oil} spanning 0.5 to 1.0 (i.e. 50 to 100% of net positive growth directed to oil). We initiate the experiments with C3s of 1.2 to 1.5 mm prosome length. Because oil accumulation occurs during spring in the Yellow Sea, we set temperatures within the range of 10 to 20°C, and food concentration to between 100 and 500 µg C l^{-1}, consistent with ocean conditions. Oil sac volume as a fraction of total body volume (i.e. OSV) is recorded at 2 h time steps. Fig. 7 shows the distribution of simulated OSV in C5s for different val-

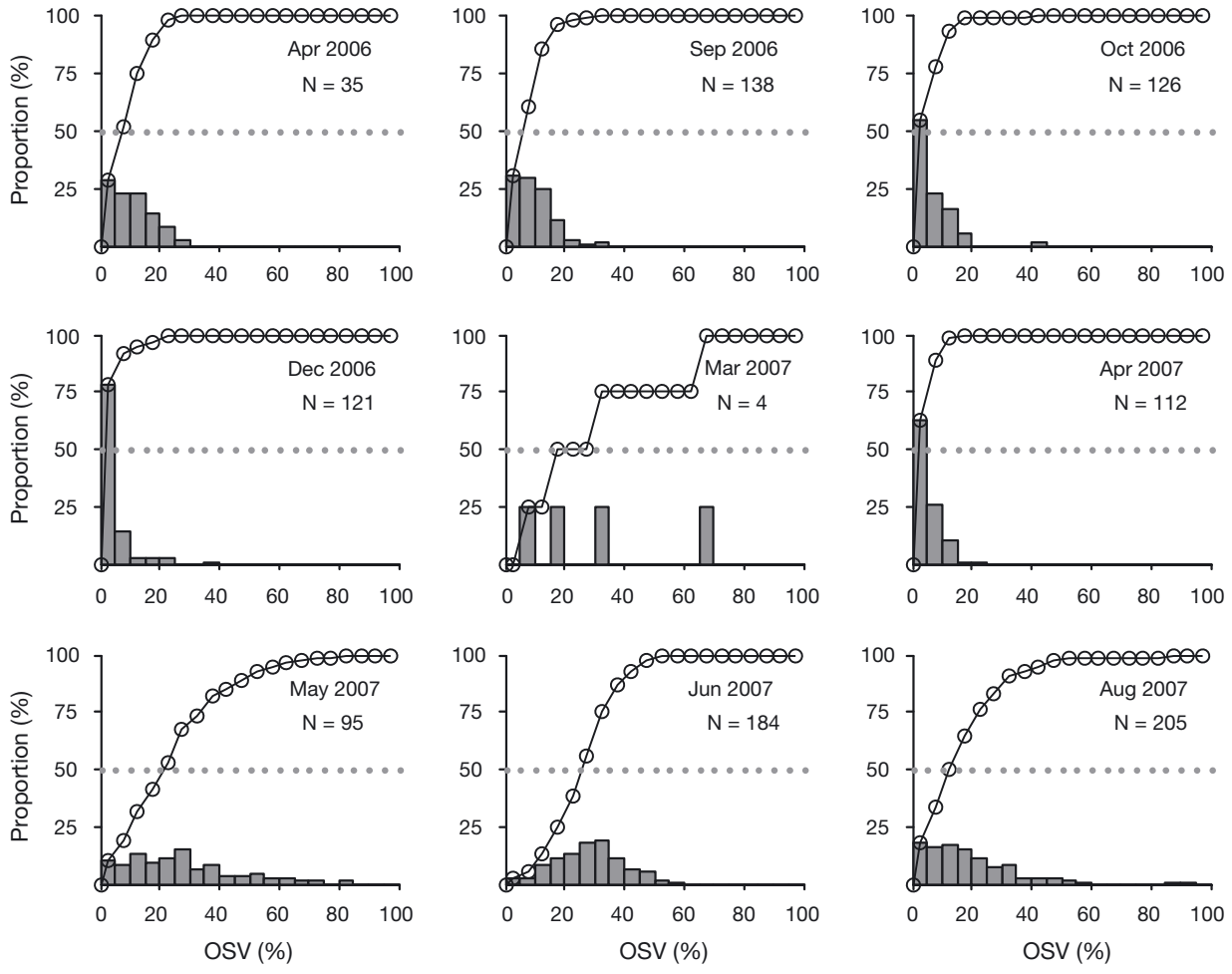

Fig. 6. *Calanus sinicus.* Seasonal variation in the distribution of oil storage volume (OSV) ratio (%) of C5s in the continental shelf area of the Yellow Sea, redrafted from Sun et al. (2011a). The bar chart shows the proportion of individuals with OSV ratios within each 5% interval; the line shows the cumulative distribution. Month and year of sampling and sample size is shown in each plot; the small sample size in Mar 2007 means that this data is not reliable. Dotted line: 50% cumulative distribution (median OSV)

ues of f_{oil} and a range of experienced temperatures. The distribution of OSV is approximately normal due to the influence of a range of initial lengths and a variety of temperature histories experienced by individuals in the IBM. The results suggest that $f_{oil} = 0.6$ provides a good match of simulated OSV and the OSV observations from May and June, with both having mean OSV of ~33 to 35% and significant proportions of the populations with between 20 and 44% OSV. A difference is that the model distribution is narrower, with very few C5s with <15% or >40% OSV in May and June; the field data show OSV more broadly distributed.

At some point as OSV increases during spring, approaching observed values of 25 to 40%, sufficient reserves are accumulated for C5a individuals to transition to C5d. A second set of simulations (although not IBM) are carried out to examine the effect of individual length and temperature, on the value of λ_{max}, a critical OSV value at which an individual C5a is considered to have sufficient oil reserves to enter diapause and last through the extended, 3 to 4 mo period when surface temperatures exceed 20°C. Because C5d individuals are near the bottom, the diapause duration of C5d spanning 1.6 to 3.0 mm prosome length (Zhang F et al. 2002a) is simulated at low temperatures (5 to 12°C) typical of the YSCBW. During diapause, metabolic rate is reduced to only 20% of the rate of an equivalently sized active C5s (Hirche 1983, Ingvarsdóttir et al. 1999, Han & Wang 2001). Diapause ends when OSV is reduced below 5% (i.e. λ_{min}, the minimum value of OSV in C5s during fall and winter), and the duration of diapause is recorded (Fig. 8). Across all scenarios, diapause

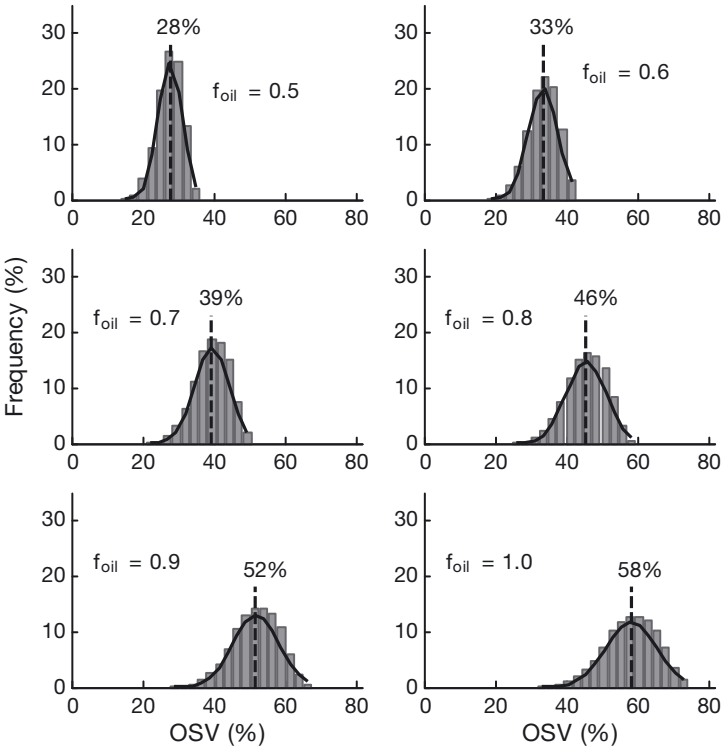

Fig. 7. *Calanus sinicus*. The distribution of oil storage volume (OSV) ratio (%) of C5s at different oil growth rates (f_{oil}) from a springtime simulation (see 'Lipid storage and diapause' in the text for details). Bars: modeled frequency distribution of OSV; solid line: fitted normal distribution; dashed line: mean OSV

duration is distributed between 45 and 160 d, and diapause can last 2 to 4 mo at 8°C, the mean temperature of YSCBW, when the λ_{max} values range from 25 to 40%. Observations of diapause duration (Pu et al. 2004b) revealed that the population of *C. sinicus* can survive for 3 to 4 mo in YSCBW, until the thermocline disappears in late October. Therefore, we consider that the λ_{max} value should be >30%. The 2 diapause simulations together suggest that 60% of the carbon growth during the later copepodite stages goes to oil storage, and that lipid-based physiological control of diapause entry occurs when the OSV exceeds 35% of the individual's body volume (λ_{max}). Diapause ends when OSV in C5d is reduced below 5% of body volume (λ_{min}), or earlier if summer stratification breaks down. Under these assumptions most C5s in spring obtain sufficient lipid reserves to enter into diapause and survive the summer in the YSCBW.

APPLICATION OF THE MODEL

The IBM of *Calanus sinicus* is applied in 1 dimension to a site located at 35°N, 123°E in the central Yellow Sea. Ideally, a complete seasonal cycle of vertical profiles of the tem-

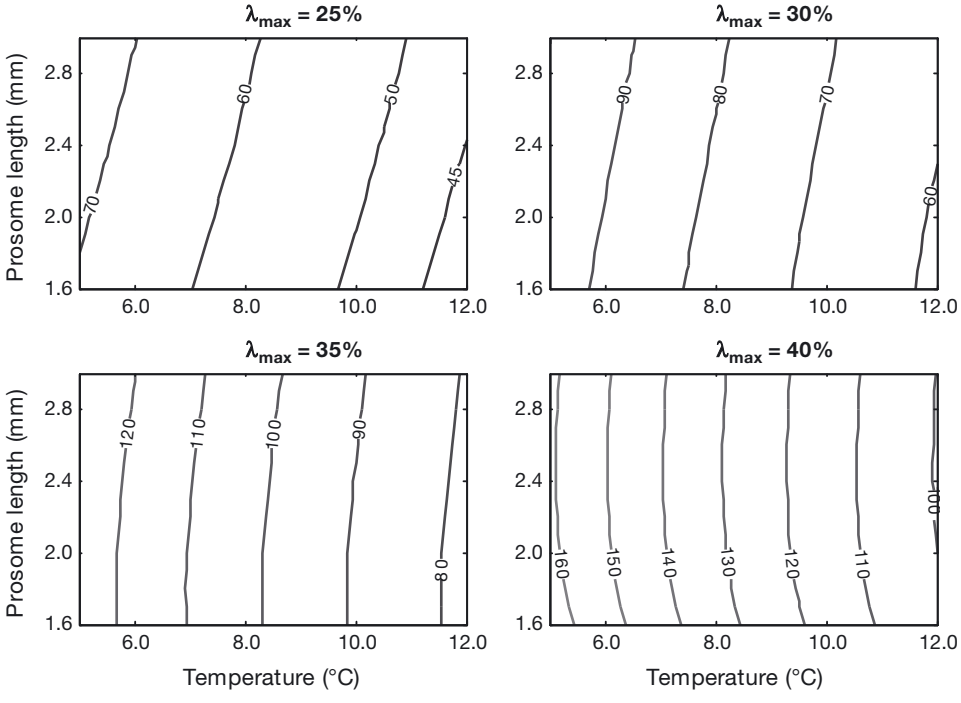

Fig. 8. *Calanus sinicus*. Effect of temperature and C5 prosome length on the duration (d) of diapause by C5 individuals (contour lines), for different values of λ_{max}, i.e. the oil storage volume (OSV) value at which a C5 individual is considered to have sufficient oil reserves to enter diapause

perature and food forcing fields would be available from the central region of the Yellow Sea for forcing the IBM. While temperature data are reasonably well known, the seasonal cycle of chl *a* is incomplete both vertically and seasonally. Springtime near surface chl *a* estimates are known from prior cruises to the region, along with a few profiles (Huo et al. 2008), and August is known to have little food at any depth (Pu et al. 2004a,b, Wang et al. 2003), but potential food concentration and its distribution during the remainder of the year are poorly known. Climatological data and chl *a* concentration from the coupled biophysical model results of Zhao & Guo (2011) provide the physical and food forcing to the IBM, respectively. The hydrodynamics are from a nested Princeton Ocean Model (Guo et al. 2003) with horizontal resolution of 1/18° and 21 sigma vertical levels in the East China Seas. The biological model is modified from NORWECOM (Aksnes et al. 1995), and includes dissolved inorganic P, N, and Si, 2 phytoplankton (diatoms [DIA] and flagellates [FLA]), and organic detritus and biogenic silicate detritus. In the present model, the summed chl *a* concentration of diatoms and flagellates is used as food in the IBM of *C. sinicus*.

The model is initialized on 1 January with 2000 adult females m^{-2}, distributed uniformly with depth (Wang 2009). Each female weighs 100 µg C. All state variables are integrated and recorded at 2 h time steps. The model achieves a steady annual cycle after 5 yr; the result from Year 5 is analyzed and shown in the 'Results' section.

The physical and food environment

According to the coupled biophysical model results of Zhao & Guo (2011), the station in the central Yellow Sea has a strong annual cycle of temperature and chl *a* (Fig. 9). The water column is vertically isothermal from January to March; weak stratification begins in April, and the thermocline intensifies at 10 to 20 m depth in late May. The period of strongest vertical stratification is defined here as when the maximum vertical temperature gradient exceeds 0.2°C m^{-1}, and spans from late May to mid-October (indicated by heavy dark line showing location of the steep gradient in temperature in Fig. 9). During this period, the depth of the

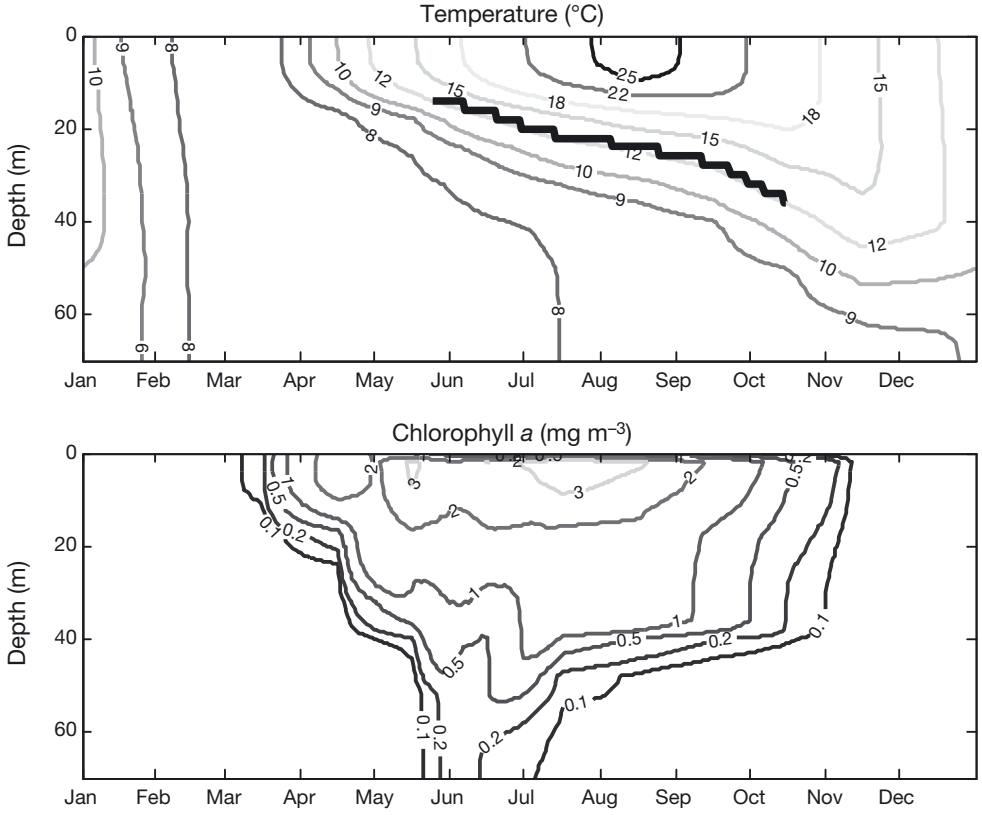

Fig. 9. *Calanus sinicus*. Depth profiles of annual cycles of temperature (°C; contour lines in top panel) and chl *a* (mg m^{-3}; bottom panel) at a station in the central Yellow Sea. The bold black line in the top panel shows the depth of the base of the thermocline during summer when $(\delta T/\delta z)_{max} > 0.2$°C m^{-1}

thermocline progressively deepens to almost 40 m, surface temperatures warm to >25°C, with the upper 10 m temperatures >20°C from late June to mid October, and temperatures below the thermocline are 8 to 10°C, typical of YSCBW. Vertical stratification weakens in October and deep mixing dominates from November to April.

Chl *a* concentration during the vertically isothermal months (November to March) is <0.1 mg m^{-3} at all depths. In early spring, chl *a* in the upper 10 m increases to ~1 mg m^{-3} by late March, and is 2 to 3 mg m^{-3} through most of the period April to July. Chl *a* concentration below the mixed layer during the most stratified summer season is much (10 to 50%) lower than surface chlorophyll.

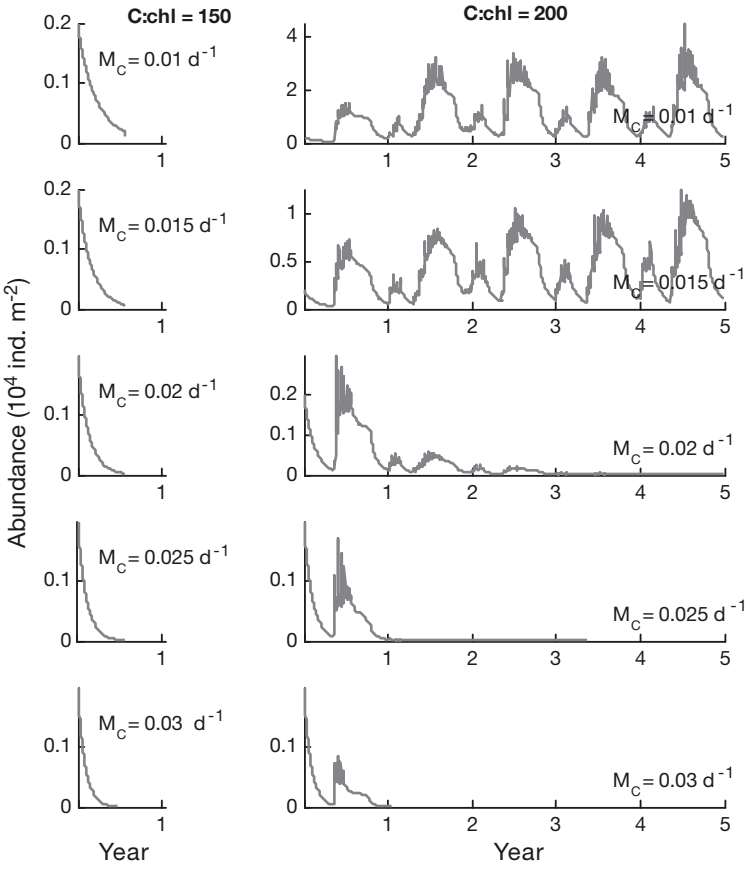

Fig. 10. *Calanus sinicus.* The annual variation of population abundance (ind. m^{-2}) for 5 routine mortality rates (M_C) of immature copepodites (0.01 to 0.03 d^{-1}) and 2 carbon-to-chlorophyll conversion (C:chl)ratios: 150 (left) and 200 (right). Populations persist for multiple years only in scenarios having low mortality rates and high C:chl ratios

Parameters used to conduct the IBM simulations

In 'Simulations for parameter estimation' above, we described several parameters ($\varphi_{I,i}$, φ_R, f_{oil}, λ_{max}, λ_{min}) that are estimated by comparing laboratory based experiments with simulations of those experiments, or by simulating observed seasonal patterns of individual lipid content. Those parameter estimates are obtained independently of information on the seasonal cycle of the abundance of *Calanus sinicus* in the central Yellow Sea. Here, we briefly describe the carbon-to-chlorophyll conversion ratio (C:chl), and 3 mortality parameters of the model which require iterative tuning to obtain good agreement between model and observations.

The routine mortality rate for the 3 stage groupings (i.e. M_N, M_C and M_A) are difficult to know since no field work has directly estimated these for *Calanus sinicus*, as has been done for *C. finmarchicus* elsewhere (Ohman & Hirche 2001, Ohman et al. 2004, 2008). Here we assume that the routine mortality of immature copepodites is identical to that of adult females ($M_C = M_A$) and half that of naupliar stages ($M_C = 0.5 \times M_N$). This simplifies the problem to tuning a single mortality parameter (see Supplements 1 & 2).

For the present simulations, estimates of total chl *a* concentration from a coupled model (Zhao & Guo 2011) are used to specify the depth and temporal abundances of prey items for *Calanus sinicus*. In general, C:chl ratios of 30 to 150 are typical of phytoplankton cultured under a range of nutrient and light conditions (Cloern et al. 1995). Simulations executed to examine *C. sinicus* population dynamics in the Yellow Sea with seasonally constant C:chl ratios ranging from 70 to 200 are entirely unsuccessful in allowing long-term (i.e. multi-year) persistence of *C. sinicus* in the central Yellow Sea for a range of mortalities (M_C = 0.01 to 0.03 d^{-1}; Fig. 10). Clearly, there must be additional sources of particulate carbon prey that does not contain chlorophyll consumed by *C. sinicus*, or they would not be able to persist in the central Yellow Sea, as they clearly do. This result suggests that *C. sinicus,* which are known to feed omnivorously on microzooplankton (Yang 1997, Huo et al. 2008), must be relying on animal food to satisfy their metabolic and growth requirements. We do not have data on the biomass density of such prey organisms through space and time. However, recent research on a microbial loop ecosystem model (Zhang et al. 2012) revealed that

'small zooplankton', most likely microzooplankton, generally follow the same seasonal pattern as phytoplankton. Therefore, we assume that the Yellow Sea has an amount of carbon prey in small heterotrophs equal to or exceeding that in chlorophyll containing organisms, and a substantial portion of the prey of *C. sinicus* are non-chlorophyll containing particles. We simulate the seasonal and depth contributions of these non-chlorophyll prey by inflating the C:chl ratio to a value (250) that supports persistent multi-year growth and development of *C. sinicus* in the Yellow Sea, when routine mortalities M_N, M_C and M_A are set to be 0.04, 0.02 and 0.02 d^{-1}, respectively. The doubling of C:chl is consistent with results reported recently on the fraction of phytoplankton carbon contribution to total particulate carbon (Sathyendranath et al. 2009).

RESULTS

Calanus sinicus population dynamics in the central Yellow Sea

Fig. 11 shows the seasonal variation of abundance, biomass and population structure of *Calanus sinicus* from the IBM simulation. As shown in the top panel, *C. sinicus* abundance peaks in late May and again in early December. The abundance of C5s and adults remain low in winter and spring; subsequently the abundance of C5s increases rapidly in June to July and remains high until early October. In these months, most *C. sinicus* are present as C5 (most of them in diapause), as shown in the bottom panel. Compared to C5s, the adult abundance varies little seasonally, except in early November, when the C5s in diapause mature to adults. The middle panel shows that the biomasses of the entire population and C5s both reach their maximum in July, and the biomass of adult females peaks in November.

The simulation shows that there are 2 peaks in abundance per year. The first peak occurs in April–May, when the phytoplankton blooms at the surface, and eggs and nauplii dominate the population. The high chl *a* concentration promotes the reproduction of females, and supplies more energy to all life stages, enhancing growth and survival. The second period when eggs and nauplii dominate occurs in December–January. Because chl *a* concentration after mid-November is low throughout the entire water column, reproduction—leading to the dominance of young stages in December–January—is derived from eggs produced using residual lipid stores available after C5 diapause terminates. As described, the C5s in diapause metabolize the oil reserves accumulated in spring for over-summering and, when diapause ends, residual oil stores, if any, are converted into egg production.

The abundances of different generations of eggs, C5s and females are shown in Fig. 12. Generation G0 represents C5s and adults that developed from eggs produced in the prior year. The population progresses through 3 generations in the year. The G1 population is produced by G0 females from January to July with peak abundance in April–May. The G2 generation from eggs laid by G1 females first

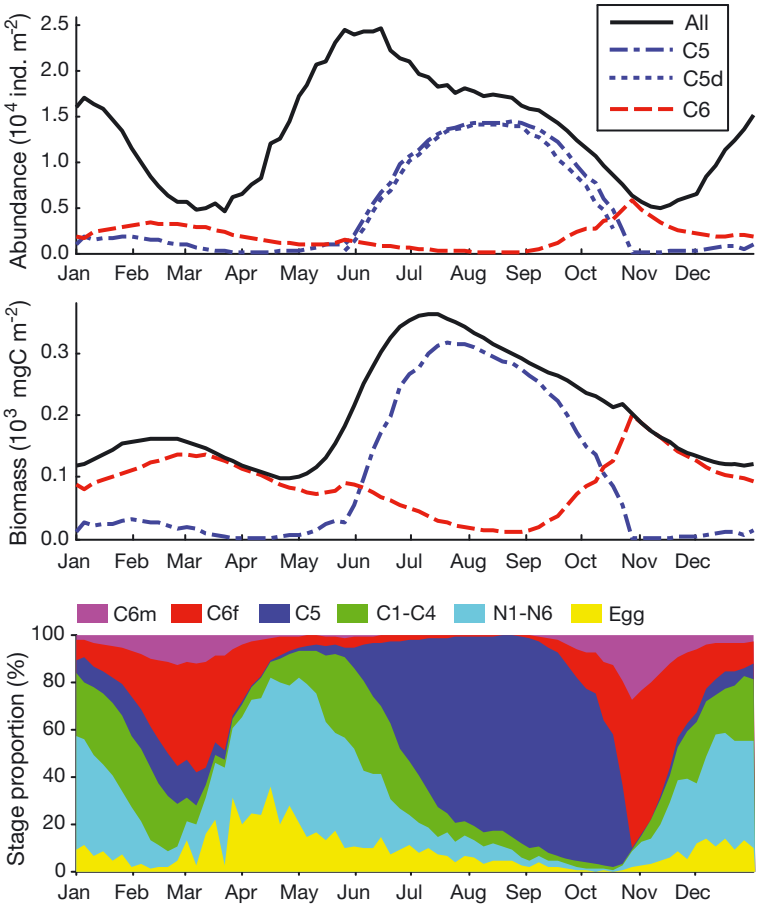

Fig. 11. *Calanus sinicus*. The seasonal variation of abundance, biomass and population structure from Year 5 of the simulation. Carbon-to-chlorophyll conversion (C:chl) ratio = 250. Routine mortality rates — nauplii: 0.04, copepodites and adult females: 0.02. N1 to N6: naupliar stages; C1 to C5: copepodite stages; C6m: adult males; C6f: adult females

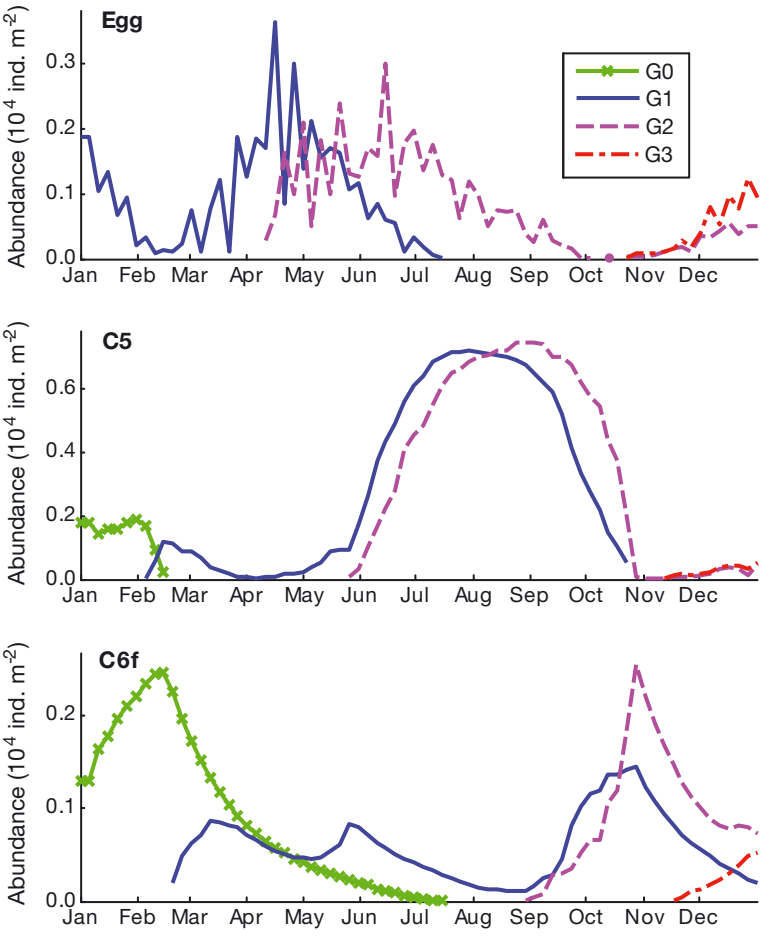

Fig. 12. *Calanus sinicus.* The seasonal variation of abundance of eggs, C5s and adult females of different generations from the model simulation. Successive generations are labeled as G0 (individuals produced in prior year) through 3 generations produced in the shown year (G1 to G3)

appears in April and remains through December. As shown in Fig. 12, the G3 generation first appears in November. Due to rapid growth and shorter generation times in spring, there is substantial overlap of the G1 and G2 populations at the C5 and C6f stages.

Synthesizing these results, the conclusion is that the modeled population mainly consists of the G1 and G2 generations of eggs and nauplii in the first (springtime) population bloom. The earliest G1 eggs, laid before mid-February, are able to mature directly to C6, bypassing an extended diapause period, and reproduce prior to the advent of seasonally adverse conditions in the summer, but most of the eggs laid after February do not reach C6 to reproduce prior to the seasonal warming, and do not reproduce until November, if at all. Thus, eggs produced in November and December are G2 and G3 offspring of *Calanus sinicus* adults from G1 and G2, respectively.

Comparison of model simulation to field observations

Direct comparison of model results to field observations is complicated by there being few prior studies that have documented the seasonal abundance and stage structure of *Calanus sinicus* in the Yellow Sea (Table 2). The few field observations available for comparison with the model vary greatly in quality (completeness of stage structure information, and temporal resolution). Chronologically, these data are, first, a time series of *C. sinicus* abundance collected from the Bohai Sea, the Yellow Sea and the East China Sea from September 1958 to December 1959. The monthly mean abundances of different stages were recorded and the seasonal variations of generations interpreted in each of these regional seas (Chen 1964, Cheng et al. 1965, Lin & Li 1984). Here, we compare our model results only to the *C. sinicus* observations from the southern Yellow Sea region (Chen 1964). A second source is biomass data of *C. sinicus* from May, August and October 1982 cruises in the Yellow Sea (Yang & Xu 1988). More recently, *C. sinicus* abundance data were col-

Table 2. *Calanus sinicus.* Summary of observations in the Yellow Sea

Date(s)	Area	Factors studied	Source
Sep 1958–Dec 1959	Southern Yellow Sea	Abundance, generations	Chen (1964)
May/Aug/Oct 1982	The Yellow Sea	Biomass	Yang & Xu (1988)
Aug 2001	Continental shelf of Yellow Sea	Abundance	Pu et al. (2004a)
Aug 2002	Continental shelf of Yellow Sea	Abundance	Pu et al. (2004b)
Sep/Dec 2006; Mar/May/Aug 2007	Southern Yellow Sea	Abundance, generations	Wang (2009)
Jun 2007	The Yellow Sea	Abundance, generations	Wang (2009)

lected along a continental shelf section of the Yellow Sea in August of 2001 and 2002 (Pu et al. 2004a,b), from 5 cruises on a section in the southern Yellow Sea in September, December of 2006 and March, May and August 2007 (Wang 2009) and a cruise in the Yellow Sea in June 2007 (Wang 2009).

The seasonal pattern of abundance for 4 stage groupings (eggs and nauplii, early copepodites, C5s, adults) of *Calanus sinicus* from observations (Chen 1964, Pu et al. 2004a, Pu et al. 2004b, Wang 2009) and simulations are shown in Fig. 13. The simulation is consistent with documented egg and naupliar abundances, except for one June observation. The timing of the seasonal peak in C1 to C4 agrees well with the observations, although the simulated abundances of these early copepodite stages are higher than observed abundances in December–January (Chen 1964), and slightly higher than in May (Chen 1964, Wang 2009) and June (Chen 1964). Abundances of C5s from the simulations are higher than observations in summer, especially the observations from the 1950s (Chen 1964). Observations by Wang (2009) suggest an earlier May peak of C5s, but observations from other years are consistent with the model peak in midsummer. Differences in timing may result from comparisons of a single simulated year with data collected from multiple (5) years. The abundance of adults remains relatively steady during the annual cycle, except for one June observation; there is weak evidence, from relatively few years of sampling, of lower adult abundance in January–March, and perhaps higher abundances during April–August. This pattern is not found in the simulation, which shows higher abundances in January–February and September–October than are reported in the data. Overall, even without specific seasonal tuning, the model is able to simulate the seasonal pattern of most stages (except the adults), and also shows abundance patterns that are consistent with most of the observations.

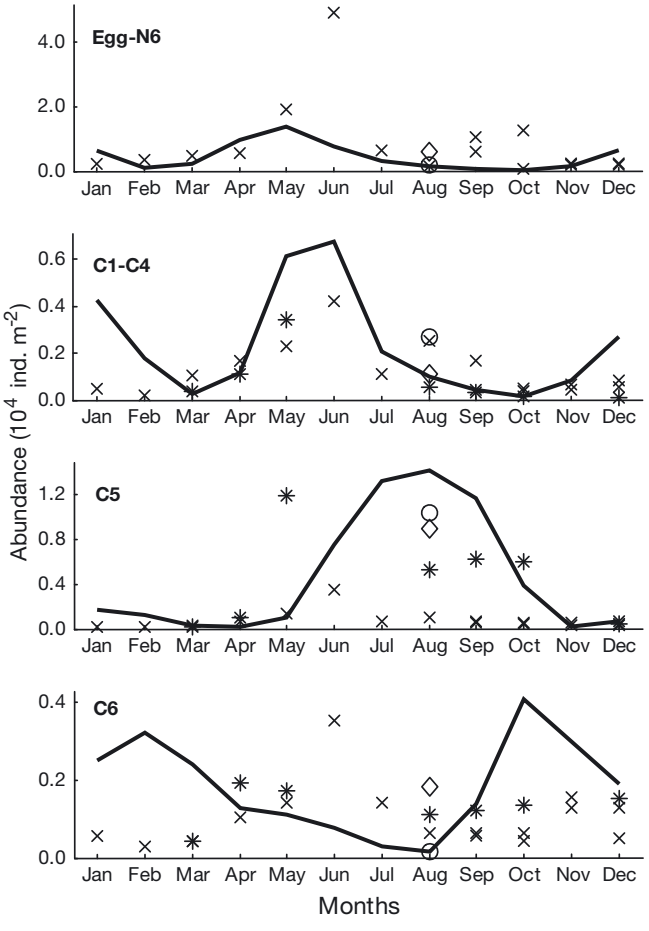

Fig. 13. *Calanus sinicus.* Observed and simulated abundances (10^4 ind. m^{-2}) in the central Yellow Sea. Observations: (×) Chen (1964); (◇) Pu et al. (2004a); (○) Pu et al. (2004b); (✳) Wang (2009). Simulated values (solid lines) are shown for (from top to bottom) eggs and all nauplii, early copepodites (Stages C1 to C4), C5s, and adults

Compared to stage-specific abundances, fewer directly measured stage-specific biomass data are available. Yang & Xu (1988) analyzed the population biomass of *Calanus sinicus* from different regions of the Yellow Sea in May, August and October. We compare observations of population biomass of *C. sinicus* in the southern Yellow Sea with our simulations. Total (all stages combined) biomass is highest in May and August (Fig. 14). The model reproduces the overall seasonal pattern of population biomass reasonably well, although it under-predicts the seasonal peak magnitude. Neither Pu et al. (2004a,b) nor Wang (2009) provide direct estimates of population biomass. However, Pu et al. (2004a,b) measured the mean weights of C5s and females, which when combined with the abundance data allow the biomass of C5s and females to be estimated. Likewise, Wang (2009) measured the mean body lengths of C5s and females, which we use to calculate the mean weight of C5s and females using a length-weight relationship (Uye 1988) to obtain stage-specific biomass for C5s and adult females. Overall, the simulated model biomass of C5s and females are seasonally similar to the sparse seasonal biomass observations of C5s and females, except the simulated increase in biomass of females during January to March occurs earlier than the observations suggest (Fig. 14).

We compare the duration of each *Calanus sinicus* generation from the simulation with observations of generation times and cohort structure (Chen 1964, Wang 2009; Table 3). The population simulation

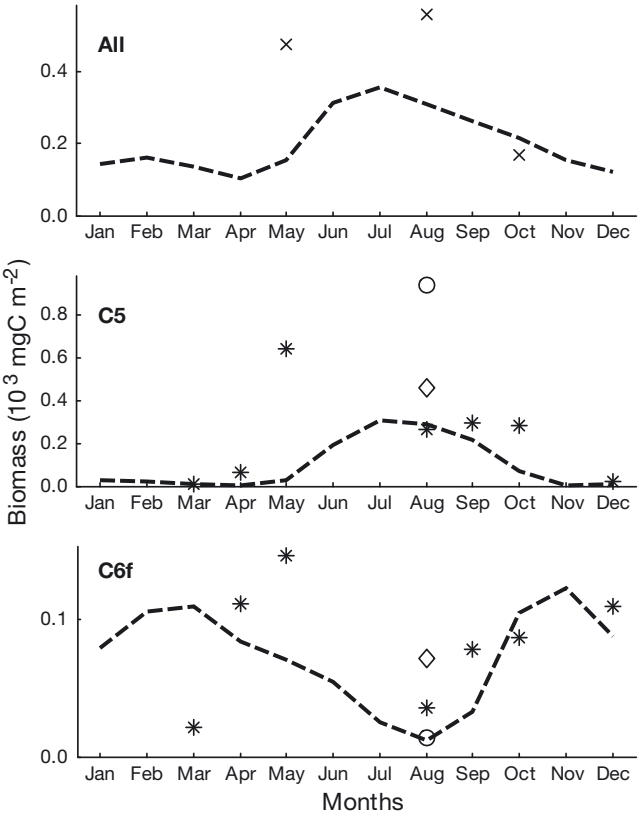

Fig. 14. *Calanus sinicus.* Observed and simulated biomass (10^3 mg C m^{-2}) in the central Yellow Sea. Observations: (×) Yang & Xu (1988); (◇) Pu et al. (2004a); (○) Pu et al. (2004b); (✳) Wang (2009). Simulated values (dashed lines) are shown for all stages (top), C5s (middle) and adult females (bottom)

shows that G1 appears as early as the result suggested by Chen (1964), and that G2 begins in early April, between the proposed time of G2 and G3 reported by Wang (2009). The simulated dynamics produce generations where the over-summering population is comprised of C5s from both G1 and G2. The timing of G3, which appears in late October in the simulation, is consistent with the interpretation by Chen (1964).

Sensitivity analysis

Simulations were done to quantify the sensitivity of model results to 10% increases and decreases from the base parameter value for specific parameters that are least constrained by empirical observations: f_{oil}, λ_{max}, the metabolic rate ratio of C5d to C5a (k_d), f_{O2E}, and the mortality rates M_N, M_C and M_A. RMS abundance deviations were calculated and standardized by several stage-based or seasons (whole-year population, spring population, population of diapause C5 and winter population; see Fig. 15). The results show that, for the whole-year population and the spring population, abundance is most sensitive to the values chosen for f_{oil} and M_A. This is expected, since f_{oil} is important in controlling the accumulation of lipid, which later indirectly influences gonad reserve accumulation when residual lipid after maturation to C6 is converted into gonad, and M_A directly affects the abundance and reproduction of females. Parameter f_{oil} is also the most sensitive parameter controlling abundance of diapausing C5s, because of its important role in determining lipid accumulation permitting successful diapause; other parameters that influence the duration of diapause, λ_{max} and k_d, are more robust. For the winter population, the model is sensitive to the respiration of C5d, which is strongly influenced by k_d, the ratio of diapause to active C5 respiration that determines the amount of residual lipid immediately available for egg production in early

Table 3. *Calanus sinicus.* Observations and model simulation of population generations in the Yellow Sea: number of generations per year, timespan and duration of successive generations (G1 to G4), generations in diapause

Source	No. of generations yr^{-1}	Generation (timespan)	Duration (mo)	Generations in diapause
Chen (1964)	3	G1 (Mar/Apr–Jul/Aug)	4–5	Mainly G2, possibly with G1
		G2 (Jul/Aug–Oct)	2–3	
		G3 (Oct–Dec)	2	
Wang (2009)	3–4	G1 (Jan–Mar)	2	Mainly G3 & G4, possibly with G2
		G2 (Mar–Apr)	1	
		G3 (Apr–May)	1	
		G4 (May–Dec)	6	
Model simulation (this study)	3	G1 (Jan–early Apr)	3 (generations for G1 simulated)	Mainly G1 & G2
		G2 (early Apr–late Oct)	6 (generations for G2 simulated)	
		G3 (late Oct–Dec)	2 (generations for G3 simulated)	

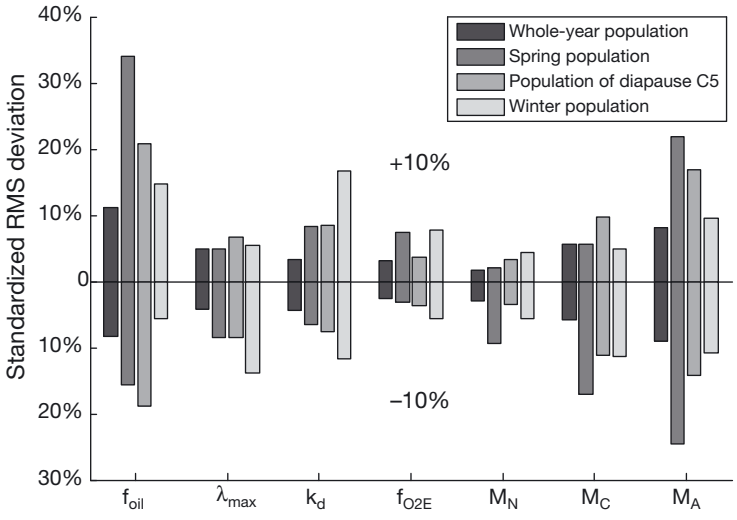

Fig. 15. *Calanus sinicus.* Sensitivity of modeled abundances to selected parameters, estimated as the root mean square (RMS) deviation with parameters increased and decreased by 10% from the base run, standardized by the mean abundance of population in different periods (whole-year population, spring population, population of diapause C5s and winter population). The 7 parameters examined are the fraction of growth directed to lipid (f_{oil}), the lipid threshold (λ_{max}), the metabolic rate ratio between active and diapausing C5 stages, i.e. C5d:C5a (k_d), the fraction of lipid used to produce eggs (gonads) (f_{O2E}), and the mortality rates of nauplii (M_N), copepodites (M_C), and adults (M_A)

winter. Among these selected parameters, f_{O2E} and M_N are the 2 least sensitive parameters to population for all standardizations.

DISCUSSION

As the first individual-based model of *Calanus sinicus*, our model successfully parameterizes the development, growth and reproduction of *C. sinicus* based on laboratory rate measurements and *in situ* observations. Where possible, we have tried to calibrate the least constrained parameters, mostly relating to individual lipid dynamics, using independent field observations. The IBM simulation shows that the population of *C. sinicus* in the central Yellow Sea increases dramatically in April–May and December. The spring increase is the greater; it includes the 1st and 2nd generations of *C. sinicus*, and is mostly dependent on the phytoplankton bloom in spring. The population increase in December–January is fueled by newly matured adult females in fall allocating residual lipids to egg production. The modeled population biomass of *C. sinicus* reaches its annual maximum in summer, when C5d are the majority of the population. The results suggest that the population of *C. sinicus* may complete 3 generations in 1 yr, and that the over-summering population consists of C5s from both G1 and G2. The seasonal diapause, which is likely initiated and terminated based on a lipid accumulation and temperature-dependent metabolism, enables the *C. sinicus* population to persist over multiple years in the central Yellow Sea. These results improve our understanding of the mechanism of diapause of *C. sinicus*; diapause has only been studied with numerical models for *C. finmarchicus* in the North Atlantic (Johnson et al. 2008, Maps et al. 2012).

The IBM simulation of *Calanus sinicus* bioenergetics and population dynamics is able to replicate many observed patterns of seasonal variation of population abundance, biomass and generation, and is able to describe the responses of population dynamics to the changes of physiological actions of individuals under environmental variation. However, the model is not able to simulate the seasonal patterns of adult abundance, possibly because of the difference between observation periods and areas, the neglect of horizontal advection, and failure to allow seasonal variation in some basic vital rates, such as mortality. One of the core data sets, that of Chen (1964), is based on observations further south in the Yellow Sea than the YSCBW region that is the focus of the model. Horizontal advection, which is not considered in the 1-dimensional simulation, might be important because observations of population dynamics suggest that the central YSCBW region may be an over-summering refuge for *C. sinicus* that recolonize adjacent Yellow Sea regions (Yin et al. 2013). In addition, the model uses simplified population dynamics, in the sense that C:chl ratios, mortality rates and other parameters were not allowed to vary seasonally. While seasonal variation might have provided better agreement with observations, it likely would have resulted in over-fitting the model relative to the few datasets available for comparison.

Surprisingly, the amount of seasonally complete data available to describe the stage-specific abundance, biomass and generation times of *Calanus sinicus* in the central Yellow Sea is quite limited, especially for a copepod that is large and reasonably successful in this regional sea, and is one of the species that dominates the zooplankton biomass. The relatively large body size of *C. sinicus* compared to the other common copepods of the Yellow Sea, and the ability to sequester significant lipid stores to with-

stand the very adverse hot summer surface temperature through C5 diapause, are key to the relative dominance (~80% of total copepod biomass) of this species. Batchelder et al. (2013) describe the important role of winter conditions and events for preconditioning subsequent spring-summer mesozooplankton population dynamics in several coastal marine ecosystems. This suggests that further field investigations of the distribution, stage structure, abundance and biomass over the full annual cycle, with ancillary observations of physiological rates and condition (e.g. lipid stores; see Sun et al. 2011a) would be of value for understanding the dynamics of *C. sinicus* in the Yellow Sea. The recently published papers from the China GLOBEC/IMBER (Integrated Marine Biogeochemistry and Ecosystems Research) studies of late winter to early summer in 2007 and 2009 (e.g. Li et al. 2013, Ning et al. 2013, Tang et al. 2013) are a good start, but they fall short of documenting ocean conditions and ecosystem structure throughout the full annual cycle. They do greatly increase the number of observations of prey fields suitable for ingestion by *C. sinicus* in the YSCBW region of the Yellow Sea, and provide an improved basis for assessing coupled biophysical models or for directly estimating *in situ* prey fields. The GLOBEC/IMBER studies indicate that chl *a* concentrations are spatially patchy in most months, but that the highest chl *a* concentrations occur in spring. Sun et al. (2011b) summarized depth integrated chl *a* concentrations from 8 cruises between April 2006 and August 2007 (see also Huo et al. 2012). They reported (Table 3 in their paper) the highest depth averaged chl *a* for spring (mean [range] 1.4 [0.3 to 5.6] mg chl m^{-3}), with lower values for summer (0.5 [0.04 to 4.9]), autumn (0.7 [0.06 to 2.9]), and winter (0.9 [0.5 to 1.7]). This pattern differs from the Zhao & Guo (2011) seasonal cycle of chl *a* provided to *C. sinicus* in the present model in having lower chl *a* concentrations, especially at the surface (data not shown here) during summer, and higher chl *a* concentrations during autumn and winter. The discrepancy in summer chl *a* concentrations may not matter, because in our model the highest chl *a* values are in the upper mixed layer after the intense stratification begins, which is excluded to *C. sinicus* foraging in our simulation. However, the data suggest that there may be 2 to 3 times more chl *a* in autumn and up to 10 times more chl *a* in winter than we use; the effect in autumn may be compensated by the high C:chl ratio we use, but the winter food levels in the YSCBW region in the recent GLOBEC/IMBER reports suggest we underestimate food levels by a factor of 2 to 3.

The parameterizations of the model also need improvement, especially in the C:chl ratio, the proportional allocation of net growth to lipid, and specification of mortality coefficients. Firstly, the C:chl ratio used is seasonally constant and relatively high, based on the prey concentrations required to enable long-term persistence of *Calanus sinicus* in the central Yellow Sea. The bioenergetic processes and other controlling variables (such as temperature and individual weight-based dependences) for ingestion, respiration, growth and development are well constrained by reliable independent observations (e.g. Uye 1988, Ikeda et al. 2001). The relatively high C:chl ratio applied to chl *a* is imposed based on the assumption that the particle feeding *C. sinicus* ingest both phytoplankton and microzooplankton (ciliates and heterotrophic dinoflagellates; e.g. Huo et al. 2008). A recent study of the annual cycle of C:chl ratios in Jiaozhou Bay, a semi-enclosed embayment on the east coast of China, adjacent to the Yellow Sea, documented monthly values from ~95 to 200 (Lu et al. 2009). If similar 2-fold variation in C:chl occurs in the central Yellow Sea, it will impact the dynamics of *C. sinicus* through an impact on seasonal food concentration. Lacking data on C:chl ratios near the study site, we take a conservative approach that assumes seasonal constancy, with the level high enough to permit the observed persistence of *C. sinicus*.

Secondly, because the dynamics of lipid accumulation is important to controlling diapause and reproduction, we believe controlled laboratory experiments providing quantitative data on somatic growth and lipid accumulation, and the fate of accumulated lipids (to respiration, somatic tissues, and reproduction) would enable future tests of the lipid accumulation hypothesis, and refinement of the IBM implemented here. Our assumption that post-diapause residual lipids are invested into egg production is speculative. The only data that relate to this proposition are the results of Wang et al. (2009) on *Calanus sinicus* egg production in spring (April) and fall (October). They found that a station-specific egg production rate (EPR) was significantly explained by a regression that included mean ciliate density and chl *a* concentration (i.e. EPR increases with ambient food), but did not include mean OSV (relative oil sac volume of females). However, the April and October data included observations from both neritic and central Yellow Sea stations, and thus are not directly comparable to the simulation results here. In October, *C. sinicus* females spawned actively at neritic stations where ciliate densities and chl *a* concentrations were greatest, but no eggs were produced at stations having <0.3 mg chl *a*

m^{-3} and low ciliate densities (<500 l^{-1}) in the central YSCBW. OSV values of females from neritic and YSCBW stations in October did not differ (Wang et al. 2009). Females in our simulations did not exhibit significant autumn reproduction until November, which we attribute partly to lipid repurposing from diapause to eggs. Ideally, future experiments will quantify both the diet composition and fate of net positive growth within the later copepodite stages and lipid dynamics during maturation. In addition, the mortality rate of different life stages, and seasonal patterns of the reproduction rate both need further investigation before a better representation of mortality can be implemented in models.

In addition, the 1-dimensional model implemented here assumes that horizontal advection is not important. This assumption may be false. Ning et al. (2013) recently suggested that movement of *Calanus sinicus* between the central Yellow Sea summer environment and neritic winter environment, both of which favour survival, is the strategy that works best in sustaining *C. sinicus* populations in the Yellow Sea. While that strategy may be more optimal, the results of the 1-dimenstional simulations described here suggest that it is possible for *C. sinicus* to sustain populations year to year in the central Yellow Sea without seasonal advection linking neritic and central regions. Moreover, the lack of *C. sinicus* egg production in October is insufficient, by itself, to argue against a self-sustaining *C. sinicus* population in the central Yellow Sea.

A more thorough understanding of how *C. sinicus* populations are controlled on larger spatial scales might be accomplished by coupling an IBM of *Calanus sinicus* to a dynamic physical-ecosystem model that provides spatially resolved descriptions of hydrography and prey abundance (including phytoplankton, heterotrophic protozoans and microheterotrophic metazoans). For such model simulations to be verified will require more intensive sampling of population abundance, biomass and prey fields seasonally in different regions of the Yellow Sea.

Acknowledgements. We appreciate the support from the National Natural Science Foundation of China under contract No. 40830854 and the support from the Ministry of Science and Technology of China by the National Key Basic Research Program of China (2011CB403606). We also thank the China Scholarship Council, which supported a visit of L.W. to the College of Oceanic & Atmospheric Sciences in Oregon State University for 12 mo. H.P.B. acknowledges the US GLOBEC program, funded jointly by the National Science Foundation and National Oceanic and Atmospheric Administration for financial support. This is US GLOBEC Contribution number 734.

LITERATURE CITED

Aksnes DL, Ulvestad KB, Baliño BM (1995) Ecological modelling in coastal waters: towards predictive physical-chemical-biological simulation models. Ophelia 41:5–36

Batchelder HP, Miller CB (1989) Life history and population dynamics of *Metridia pacifica*: results from simulation modeling. Ecol Model 48:113–136

Batchelder HP, Williams R (1995) Individual-based modelling of the population dynamics of *Metridia lucens* in the North Atlantic. ICES J Mar Sci 52:469–482

Batchelder HP, Edwards CA, Powell TM (2002) Individual-based models of copepod populations in coastal upwelling regions: implications of physiologically and environmentally influenced diel vertical migration on demographic success and nearshore retention. Prog Oceanogr 53: 307–333

Batchelder HP, Daly K, Davis C, Ji R, Ohman M, Peterson W, Runge J (2013) Climate impacts on zooplankton populationdynamics in coastal marine ecosystems. Oceanography 26:34–51

Campbell RG, Wagner MM, Teegarden GJ, Boudreau CA, Durbin EG (2001) Growth and development rates of the copepod *Calanus finmarchicus* reared in the laboratory. Mar Ecol Prog Ser 221:161–183

Carlotti F, Hirche H (1997) Growth and egg production of female *Calanus finmarchicus*: an individual-based physiological model and experimental validation. Mar Ecol Prog Ser 149:91–104

Chen Q (1964) A study of the breeding periods, variation in sex ratio and in size of *Calanus sinicus* brodsky. Oceanol Limnol Sin 6:272–288 (in Chinese with English Abstract)

Cheng C, Cheng TC, Wang R, Ling Y, Gao S (1965) Ecological investigations on the zooplankton of the mackerel fishing group off Yentai-Weihai and adjacent waters. Oceanol Limnol Sin 7:329–354 (in Chinese with English Abstract)

Cloern JE, Grenz C, Vidergar-Lucas L (1995) An empirical model of the phytoplankton chlorophyll:carbon ratio: the conversion factor between productivity and growth rate. Limnol Oceanogr 40:1313–1321

Fager EW (1973) Estimation of mortality coefficients from field samples of zooplankton. Limnol Oceanogr 18: 297–301

Fennel W (2001) Modeling of copepods with links to circulation models. J Plankton Res 23:1217–1232

Gnaiger E (1983) Calculation of energetic and biochemical equivalents of respiratory oxygen consumption. In: Gnaiger E, Forstner H (eds) Polarographic oxygen sensors. Springer, Berlin, p 337–345

Guo X, Hukuda H, Miyazawa Y, Yamagata T (2003) A triply nested ocean model for simulating the Kuroshio-roles of horizontal resolution on JEBAR. J Phys Oceanogr 33: 146–169

Han X, Wang R (2001) The studies on diapause of copepods. Mark Sci 25:24–26 (in Chinese with English Abstract)

Heath M, Robertson W, Mardaljevic J, Gurney WSG (1997) Modelling the population dynamics of *Calanus* in the Fair Isle current off northern Scotland. J Sea Res 38: 381–412

Hind A, Gurney WSC, Heath M, Bryant AD (2000) Overwintering strategies in *Calanus finmarchicus.* Mar Ecol Prog Ser 193:95–107

Hirche HJ (1983) Overwintering of *Calanus finmarchicus* and *C. helgolandicus.* Mar Ecol Prog Ser 11:281–290

Ho C, Wang Y, Lei Z, Xu S (1959) A preliminary study of the formation of Yellow Sea Cold Mass and its properties. Oceanol Limnol Sin 2:11–15 (in Chinese with English Abstract)

Huo Y, Wang S, Sun S, Li C, Liu M (2008) Feeding and egg production of the planktonic copepod *Calanus sinicus* in spring and autumn in the Yellow Sea, China. J Plankton Res 30:723–734

Huo Y, Sun S, Zhang F, Wang M, Li C, Yang B (2012) Biomass and estimated properties of size-fractionated zooplankton in the Yellow Sea, China. J Mar Syst 94:1–8

Hygum BH, Rey C, Hansen BW, Tande K (2000) Importance of food quantity to structural growth rate and neutral lipid reserves accumulated in *Calanus finmarchicus.* Mar Biol 136:1057–1073

Ikeda T, Kanno Y, Ozaki K, Shinada A (2001) Metabolic rates of epipelagic marine copepods as a function of body mass and temperature. Mar Biol 139:587–596

Ingvarsdóttir A, Houlihan DF, Heath MR, Hay SJ (1999) Seasonal changes in respiration rates of copepodite Stage V *Calanus finmarchicus* (Gunnerus). Fish Oceanogr 8: 73–83

Irigoien X (2004) Some ideas about the role of lipids in the life cycle of *Calanus finmarchicus.* J Plankton Res 26: 259–263

Johnson CL, Leising AW, Runge JA, Head EJH, Pepin P, Plourde S, Durbin EG (2008) Characteristics of *Calanus finmarchicus* dormancy patterns in the northwest Atlantic. ICES J Mar Sci 65:339–350

Jónasdóttir S (1999) Lipid content of *Calanus finmarchicus* during overwintering in the Faroe-Shetland Channel. Fish Oceanogr 8:61–72

Kang HK, Lee CR, Choi KH (2011) Egg production rate of the copepod *Calanus sinicus* off the Korean coast of the Yellow Sea during spring. Ocean Sci J 46:133–143

Kattner G, Krause M (1987) Changes in lipids during the development of *Calanus finmarchicus* s.l. from copepodid I to adult. Mar Biol 96:511–518

Kwan P (1962) Some problems concerning the study of the current structure of the near-shore area of China sea. Oceanol Limnol Sin 25:30–33 (in Chinese with English Abstract)

Kwan P (1963) A preliminary study of the temperature variations and the characteristics of the circulation of the cold water mass of the Yellow Sea. Oceanol Limnol Sin 5: 255–284 (in Chinese with English Abstract)

Lee RF, Nevenzel JC, Paffenhofer GA (1970) Wax esters in marine copepods. Science 167:1510–1511

Lee RF, Hagen W, Kattner G (2006) Lipid storage in marine zooplankton. Mar Ecol Prog Ser 307:273–306

Li C, Sun S, Wang R, Wang X (2004) Feeding and respiration rates of a planktonic copepod (*Calanus sinicus*) oversummering in Yellow Sea Cold Bottom Waters. Mar Biol 145: 149–157

Li J, Sun S, Li C, Zhang Z, Tao Z (2006) Effects of single and mixed diatom diets on the reproduction of copepod *Calanus sinicus.* Acta Hydrochim Hydrobiol 34:117–125

Li C, Yang G, Ning J, Sun J, Yang B, Sun S (2013) Response of copepod grazing and reproduction to different taxa of spring bloom phytoplankton in the Southern Yellow Sea. Deep-Sea Res II 97:101–108

Lin Y, Li S (1984) A preliminary study on the life cycle of *Calanus sinicus* in Xiamen Harbour. J Xiamen Univ 23: 111–117 (in Chinese with English Abstract)

Liu T (2010) Preliminary study on the relationship between spring phytoplankton bloom and physical environment in the central Southern Yellow Sea. MS thesis, Ocean University of China, Qingdao (in Chinese with English Abstract)

Liu X, Wang Z (1991) A preliminary research on diel vertical migration of zooplankton in north Yellow Sea. Acta Oceanol Sin 13:247–253 (in Chinese with English Abstract)

Lu S, Wang X, Han B (2009) A field study on the conversion ratio of phytoplankton biomass carbon to chlorophyll-a in Jiaozhou Bay, China. Chin J Oceanology Limnol 27: 793–805

Maps F, Plourde S, Zakardjian B (2010) Control of dormancy by lipid metabolism in *Calanus finmarchicus*: a population model test. Mar Ecol Prog Ser 403:165–180

Maps F, Zakardjian B, Plourde S, Saucier FJ (2011) Modeling the interactions between the seasonal and diel migration behaviors of *Calanus finmarchicus* and the circulation in the Gulf of St. Lawrence (Canada). J Mar Syst 88:183–202

Maps F, Runge J, Leising A, Pershing AJ, Record NR, Plourde S, Pierson J (2012) Modeling the timing and duration of dormancy in populations of *Calanus finmarchicus* from the Northwest Atlantic shelf. J Plankton Res 34:36–54

McLaren IA, Corkett CJ, Zillioux EJ (1969) Temperature adaptations of copepod eggs from the arctic to the tropics. Biol Bull 137:486–493

Miller CB, Tande KS (1993) Stage duration estimation for *Calanus* populations, a modeling study. Mar Ecol Prog Ser 102:15–34

Miller CB, Cowles TJ, Wiebe PH, Copley NJ, Grigg H (1991) Phenology in *Calanus finmarchicus*: hypotheses about control mechanisms. Mar Ecol Prog Ser 72:79–91

Miller CB, Lynch DR, Carlotti F, Gentleman W, Lewis CVW (1998a) Coupling of an individual-based population dynamic model of *Calanus finmarchicus* to a circulation model for the Georges Bank region. Fish Oceanogr 7: 219–234

Miller CB, Morgan CA, Prahl FG, Sparrow MA (1998b) Storage lipids of the copepod *Calanus finmarchicus* from Georges Bank and the Gulf of Maine. Limnol Oceanogr 43:488–497

Miller CB, Crain JA, Morgan CA (2000) Oil storage variability in *Calanus finmarchicus.* ICES J Mar Sci 57: 1786–1799

Miller TJ (2007) Contribution of individual-based coupled physical-biological models to understanding recruitment in marine fish populations. Mar Ecol Prog Ser 347: 127–138

Neuheimer AB, Gentleman WC, Pepin P, Head EJ (2010) Explaining regional variability in copepod recruitment: implications for a changing climate. Prog Oceanogr 87: 94–105

Ning J, Wang M, Li C, Sun S (2013) Transcriptome sequencing and de novo analysis of the copepod *Calanus sinicus* using 454 GS FLX. PLoS ONE 8:e63741

North EW, Gallego A, Petitgas P (2009) Manual of recommended practices for modeling physical-biological interactions during fish early life. ICES Cooperative Research Report 295, International Council for the Exploration of the Sea, Copenhagen

Ohman MD, Hirche HJ (2001) Density-dependent mortality in an oceanic copepod population. Nature 412:638–641

Ohman MD, Hsieh CH (2008) Spatial differences in mortal-

ity of *Calanus pacificus* within the California Current System. J Plankton Res 30:359–366

Ohman MD, Drits AV, Clarke ME, Plourde S (1998) Differential dormancy of co-occurring copepods. Deep-Sea Res II 45:1709–1740

Ohman MD, Eiane K, Durbin EG, Runge JA, Hirche HJ (2004) A comparative study of *Calanus finmarchicus* mortality patterns at five localities in the North Atlantic. ICES J Mar Sci 61:687–697

Ohman MD, Durbin EG, Runge JA, Sullivan Atkinson BK, Field DB (2008) Relationship of predation potential to mortality of *Calanus finmarchicus* on Georges Bank, northwest Atlantic. Limnol Oceanogr 53:1643–1655

Pershing AJ, Record NR, Monger BC, Pendleton DE, Woodard LA (2009) Model-based estimates of *Calanus finmarchicus* abundance in the Gulf of Maine. Mar Ecol Prog Ser 378:227–243

Pu X (2003) Reproductive strategy of *Calanus sinicus* in the Southern Yellow Sea. PhD dissertation, The Graduate University, Chinese Academy of Sciences, Qingdao (in Chinese with English Abstract)

Pu X, Sun S, Wang X, Wu Y (2002) Effects of temperature and food supply on C5 copepodites of *Calanus sinicus* in the South Yellow Sea in summer. Oceanol Limnol Sin (Spec Issue):61–70 (in Chinese with English Abstract)

Pu X, Sun S, Yang B, Ji P, Zhang Y, Zhang F (2004a) The combined effects of temperature and food supply on *Calanus sinicus* in the southern Yellow Sea in summer. J Plankton Res 26:1049–1057

Pu X, Sun S, Yang B, Zhang G, Zhang F (2004b) Life history strategies of *Calanus sinicus* in the southern Yellow Sea in summer. J Plankton Res 26:1059–1068

Record NR, Pershing AJ (2008) Modeling zooplankton development using the monotonic upstream scheme for conservation laws. Limnol Oceanogr Methods 6:364–372

Rey-Rassat C, Irigoien X, Harris R, Carlotti F (2002) Energetic cost of gonad development in *Calanus finmarchicus* and *C. helgolandicus.* Mar Ecol Prog Ser 238:301–306

Sathyendranath S, Stuart V, Nair A, Oka K and others (2009) Carbon-to-chlorophyll ratio and growth rate of phytoplankton in the sea. Mar Ecol Prog Ser 383:73–84

Saumweber WJ, Durbin EG (2006) Estimating potential diapause duration in *Calanus finmarchicus.* Deep-Sea Res II 53:2597–2617

Scheffer M, Baveco JM, DeAngelis DL, Rose KA, van Nes EH (1995) Super-individuals a simple solution for modelling large populations on an individual basis. Ecol Model 80:161–170

Su J (2001) A review of circulation dynamics of the coastal oceans near China. Acta Oceanol Sin 23:1–14 (in Chinese with English Abstract)

Su Y, Weng X (1994) Water masses in China seas. In: Zhou D, Liang YB, Zeng CK (eds) Oceanology of China seas. Kluwer Academic, Dordrecht, p 3–26

Sun S, Wang R, Zhang G, Yang B, Ji P, Zhang F (2002) A preliminary study on the over-summer strategy of *Calanus sinicus* in the Yellow Sea. Oceanol Limnol Sin (Spec Issue):92–99 (in Chinese with English Abstract)

Sun S, Wang S, Li C (2011a) Preliminary study on the oil storage of *Calanus sinicus* fifth copepodites (C5) in the Yellow Sea. Oceanol Limnol Sin 42:165–169 (in Chinese with English Abstract)

Sun S, Tao Z, Li C, Liu H (2011b) Spatial distribution and population structure of *Euphausia pacifica* in the Yellow Sea (2006-2007). J Plankton Res 33:873–889

Tang Y, Zou E, Lie H (2001) On the origin and path of the Huanghai Warm Current during winter and early spring. Acta Oceanol Sin 23:1–12 (in Chinese with English Abstract)

Tang Q, Zhang J, Su J, Tong L (2013) Spring blooms and the ecosystem processes: the case study of the Yellow Sea. Deep-Sea Res II 97:1–3

Teague WJ, Jacobs GA (2000) Current observations on the development of the Yellow Sea Warm Current. J Geophys Res 105:3401–3411

Thornton KW, Lessem AS (1978) A temperature algorithm for modifying biological rates. Trans Am Fish Soc 107: 284–287

Uye S (1988) Temperature-dependent development and growth of *Calanus sinicus* (*Copepoda: Calanoida*) in the laboratory. Hydrobiol 167-168:285–293

Uye S, Murase A (1997) Relationship of egg production rates of the planktonic copepod *Calanus sinicus* to phytoplankton availability in the Inland Sea of Japan. Plankton Biol Ecol 44:3–11

Vidal J (1980) Physioecology of zooplankton II: effects of phytoplankton concentration, temperature, and body size on the development and molting rates of *Calanus pacificus* and *Pseudocalanus* sp. Mar Biol 56:135–146

Wang S (2009) Reproduction, population recruitment and life history of *Calanus sinicus* in the Yellow Sea. PhD dissertation, The Graduate University, Chinese Academy of Sciences, Qingdao (in Chinese with English Abstract)

Wang X, Sun S, Pu X, Zhang F (2002) The body length, weight, element composition and metabolism of *Calanus sinicus* in the Yellow Sea Cold Water Mass. Oceanol Limnol Sin (Spec Issue):45–50 (in Chinese with English Abstract)

Wang R, Zuo T, Wang K (2003) The Yellow Sea cold bottom water — an oversummering site for *Calanus sinicus* (Copepoda, Crustacea). J Plankton Res 25:169–183

Wang S, Li C, Sun S, Ning X, Zhang W (2009) Spring and autumn reproduction of *Calanus sinicus* in the Yellow Sea. Mar Ecol Prog Ser 379:123–133

Weng X, Zhang Y, Wang C, Zhang Q (1988) The variational characteristics of the Huanghai Sea (Yellow Sea) Cold Water Mass. Oceanol Limnol Sin 19:368–379 (in Chinese with English Abstract)

Yang J (1997) Primary study on the feeding of the Bohai Sea *Calanus sinicus.* Oceanol Limnol Sin 28:376–382 (in Chinese with English Abstract)

Yang B, Xu H (1988) The biomass of the principal copepods in Yellow Sea. J Dalian Fish Univ 3:35–42 (in Chinese with English Abstract)

Yin J, Zhang G, Zhao Z, Wang S, Wan A (2013) Annual variation in *Calanus sinicus* abundance and population structure in the northern boundary area of the Yellow Sea Cold Water Mass. Chin J Oceanol Limn 31: 1284–1294

Zhang F (2001) Ecological study on reproduction and growth of planktonic copepod *Calanus sinicus.* MS thesis, The Graduate University, Chinese Academy of Sciences, Qingdao (in Chinese with English Abstract)

Zhang W, Wang R, Wang K (2000) Effect of temperature on metabolic rates of *Calanus sinicus.* Mark Sci 24:42–44 (in Chinese with English Abstract)

Zhang F, Sun S, Wang X (2002a) Preliminary study on the effect of temperature and food on growth of *Calanus sinicus* in the laboratory. Oceanol Limnol Sin (Spec Issue): 19–25 (in Chinese with English Abstract)

Zhang G, Sun S, Sun Sh (2002a) Effects of diel spawning rhythm and temperature on egg production and hatching success of *Calanus Sinicus.* Oceanol Limnol Sin (Spec Issue):71–77 (in Chinese with English Abstract)

Zhang F, Sun S, Zhang G (2002b) Preliminary study on egg-laying and hatching of *Calanus sinicus* in the laboratory. Oceanol Limnol Sin (Spec Issue):10–18 (in Chinese with English Abstract)

Zhang G, Sun S, Zhang F, Liu G (2002b) Deleterious effects of temperature on the reproduction of *Calanus Sinicus* in Southern Yellow Sea in summer. Oceanol Limnol Sin (Spec Issue):85–91 (in Chinese with English Abstract)

Zhang F, Sun S, Zhang Y, Zhang W (2005) Ontogenetic diel vertical distribution of the planktonic copepod *Calanus Sinicus* in Southern Yellow Sea. Mark Sci 29:9–13 (in Chinese with English Abstract)

Zhang G, Sun S, Zhang F (2005) Seasonal variation of reproduction rates and body size of *Calanus sinicus* in the Southern Yellow Sea, China. J Plankton Res 27:135–143

Zhang G, Sun S, Yang B (2007) Summer reproduction of the planktonic copepod *Calanus sinicus* in the Yellow Sea: influences of high surface temperature and cold bottom water. J Plankton Res 29:179–186

Zhang S, Wang Q, Lu Y, Cui H, Yuan Y (2008) Observation of the seasonal evolution of the Yellow Sea Cold Water Mass in 1996–1998. Cont Shelf Res 28:442–457

Zhang L, Wang Y, Wei H, Huang B, Xiao T (2012) Establishment and validation of microbial loop ecosystem model in the Yellow Sea. Adv Mar Sci 30:457–476 (in Chinese with English Abstract)

Zhao L, Guo X (2011) Influence of cross-shelf water transport on nutrients and phytoplankton in the East China Sea: a model study. Ocean Sci 7:27–43

Editorial responsibility: Alejandro Gallego, Aberdeen, UK

Submitted: January 2, 2013; Accepted: January 8, 2014
Proofs received from author(s): April 6, 2014